Article

Neuron

# Control of Synaptic Specificity by Establishing a Relative Preference for Synaptic Partners

## Highlights

- DIP-β is necessary for proper synaptic connectivity in the *Drosophila* visual system
- DIPs-β and γ are sufficient to promote synapse formation *in vivo*
- DIP IgSF proteins are necessary for proper visual function in *Drosophila*

## Authors

Chundi Xu, Emma Theisen, Ryan Maloney, ..., Benjamin de Bivort, Jan Drugowitsch, Matthew Y. Pecot

## Correspondence

xcd0317@gmail.com (C.X.), matthew_pecot@hms.harvard.edu (M.Y.P.)

## In Brief

Xu et al. show that in the *Drosophila* visual system, DIP IgSF proteins are not necessary for synaptogenesis but regulate synaptic specificity by promoting synapses to form between specific cell types.

Xu et al., 2019, Neuron *103*, 865–877
September 4, 2019 
https://doi.org/10.1016/j.neuron.2019.06.006

CellPress

Neuron
Article

# Control of Synaptic Specificity by Establishing a Relative Preference for Synaptic Partners

Chundi Xu,[1,*] Emma Theisen,[1] Ryan Maloney,[1] Jing Peng,[1] Ivan Santiago,[1] Clarence Yapp,[2] Zachary Werkhoven,[3] Elijah Rumbaut,[1] Bryan Shum,[1] Dorota Tarnogorska,[4] Jolanta Borycz,[4] Liming Tan,[5] Maximilien Courgeon,[6] Tessa Griffin,[1] Raina Levin,[1] Ian A. Meinertzhagen,[4] Benjamin de Bivort,[3] Jan Drugowitsch,[1] and Matthew Y. Pecot[1,7,*]
[1]Department of Neurobiology, Harvard Medical School, 220 Longwood Ave, Boston, MA 02115, USA
[2]Image and Data Analysis Core, Harvard Medical School, Boston, MA 02115, USA
[3]Center for Brain Science and Department of Organismic and Evolutionary Biology, Harvard University, Cambridge, MA 02138, USA
[4]Department of Psychology and Neuroscience, Life Sciences Centre, Dalhousie University, Halifax, NS B3H 4R2, Canada
[5]Department of Biological Chemistry, HHMI, David Geffen School of Medicine, University of California, Los Angeles, Los Angeles, CA 90095, USA
[6]Department of Biology, New York University, 100 Washington Square East, New York, NY 10003, USA
[7]Lead Contact
*Correspondence: xcd0317@gmail.com (C.X.), matthew_pecot@hms.harvard.edu (M.Y.P.)
https://doi.org/10.1016/j.neuron.2019.06.006

## SUMMARY

**The ability of neurons to identify correct synaptic partners is fundamental to the proper assembly and function of neural circuits. Relative to other steps in circuit formation such as axon guidance, our knowledge of how synaptic partner selection is regulated is severely limited. *Drosophila* Dpr and DIP immunoglobulin superfamily (IgSF) cell-surface proteins bind heterophilically and are expressed in a complementary manner between synaptic partners in the visual system. Here, we show that in the lamina, DIP misexpression is sufficient to promote synapse formation with Dpr-expressing neurons and that disrupting DIP function results in ectopic synapse formation. These findings indicate that DIP proteins promote synapses to form between specific cell types and that in their absence, neurons synapse with alternative partners. We propose that neurons have the capacity to synapse with a broad range of cell types and that synaptic specificity is achieved by establishing a preference for specific partners.**

## INTRODUCTION

The formation of precise connections between neurons underlies the structural organization and function of the nervous system. In general, precise neural connectivity is established in a stepwise manner that serves to reduce the molecular complexity necessary for specifying neural connections. For example, events such as axon guidance (Huber et al., 2003; Kolodkin and Tessier-Lavigne, 2011; Tessier-Lavigne and Goodman, 1996), topographic positioning (Cang and Feldheim, 2013; Feldheim and O'Leary, 2010; Flanagan, 2006), and laminar innervation (Baier, 2013; Huberman et al., 2010; Sanes and Yamagata, 1999) target neural processes to specific locations, thereby restricting the partners available for synapse formation. Over the past several decades, progress has been made in identifying molecules that regulate these processes. However, within their local environment, neurons still face the challenge of identifying correct synaptic partners amidst many alternatives (referred to here as synaptic specificity), and how this is achieved remains poorly understood. Based on landmark studies showing that regenerating neurons have the capacity to distinguish appropriate from inappropriate synaptic targets (Langley, 1895; reviewed in Sperry, 1963), it was proposed that synaptic specificity is regulated by molecular determinants that mediate recognition between synaptic partners. A common interpretation of this idea is that recognition of the correct partners is necessary for synaptogenesis. However, few molecules have been shown to directly mediate selective interactions between synaptic partners (but see Ashley et al., 2019; Duan et al., 2014; Hong et al., 2012; Krishnaswamy et al., 2015; Mosca et al., 2012; Venkatasubramanian et al., 2019; Xu et al., 2018).

Recent biochemical, gene expression, and protein expression studies have demonstrated that the members of two subfamilies of the immunoglobulin superfamily (IgSF), the Dpr (defective proboscis retraction) family (21 members) (Carrillo et al., 2015; Nakamura et al., 2002) and the Dpr-interacting proteins (DIPs) (11 members) (Cosmanescu et al., 2018; Özkan et al., 2013), form a complex protein interaction network (Carrillo et al., 2015; Cheng et al., 2019; Cosmanescu et al., 2018; Özkan et al., 2013; Zinn and Özkan, 2017) and are expressed in a complementary manner between synaptically coupled cell types during development in the *Drosophila* visual system (Carrillo et al., 2015; Tan et al., 2015). Based on these findings, Dpr-DIP interactions are proposed to play an instructive role in regulating synaptic specificity (Carrillo et al., 2015; Tan et al., 2015). Dprs and DIPs have two or three Ig domains in their extracellular regions, respectively, and they predominantly bind heterophilically, with few exhibiting homophilic binding. Dpr-DIP complexes bear a striking resemblance to the complexes of mammalian IgSF proteins, and Dpr-DIP proteins are homologous to the IgLON protein family in vertebrates (Cheng et al., 2019; Zinn and Özkan, 2017). Dpr-DIP interactions play diverse roles in regulating the

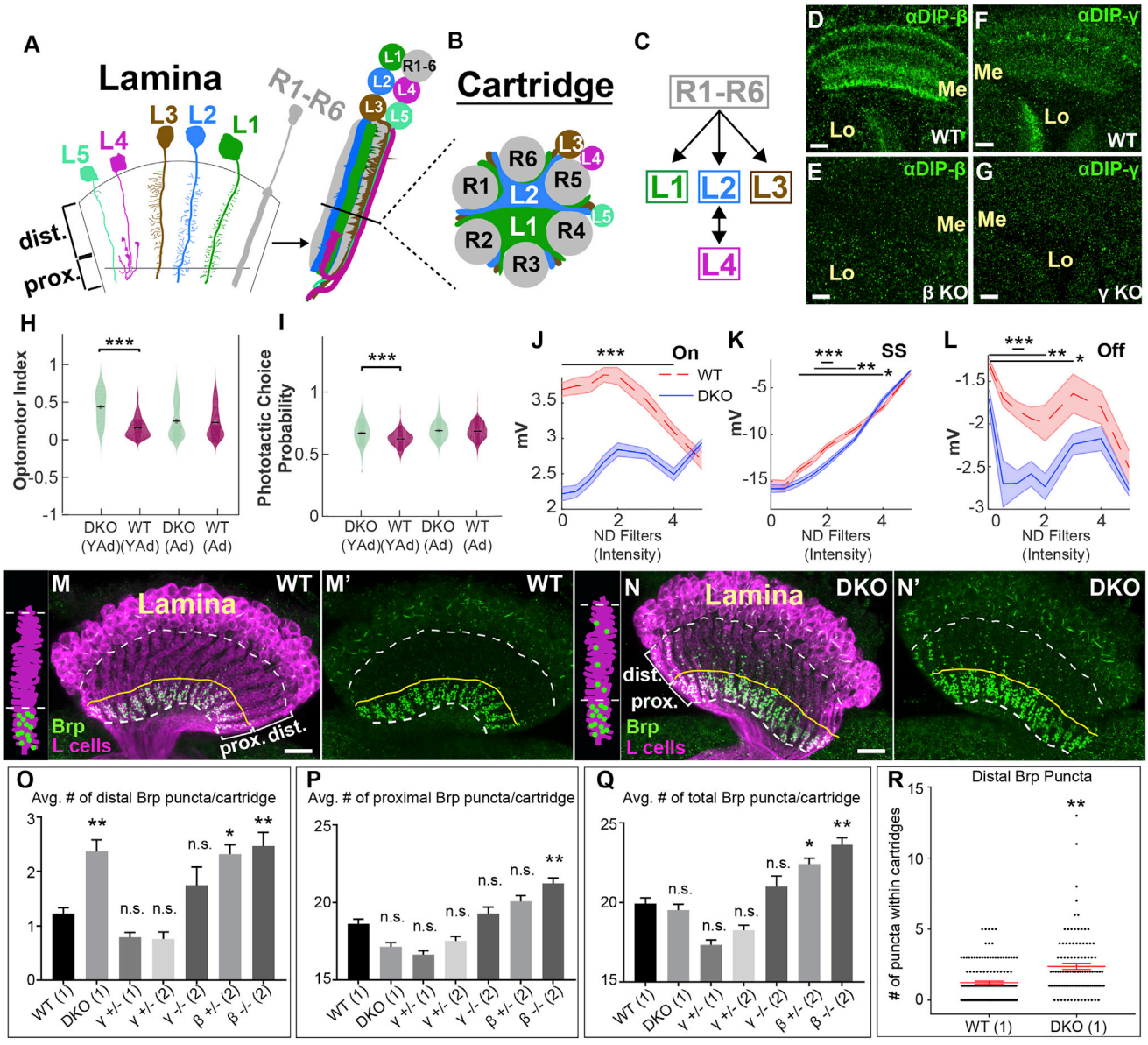


**Figure 1. DIP Proteins Are Required for Visual Function and Proper Synaptic Connectivity**

(A–C) Cellular and synaptic organization of the lamina.

(A) Longitudinal view of lamina cartridge organization.

(B) Cross-section through a lamina cartridge.

(C) Diagram of synaptic connectivity within lamina cartridges.

(D–G) Confocal images showing DIP-β (D and E) or DIP-γ (F and G) immunolabeling (green) in the medulla (Me) and lobula (Lo) neuropils at 40–48 h after puparium formation (h APF). Scale bars, 10 μm. (D and F) In wild-type flies, DIPs-β and γ are expressed in the medulla and lobula (n = 6 brains and n = 7 brains, respectively). (E and G) The expression of DIPs-β and γ in the medulla and lobula is severely reduced in flies homozygous for DIP-β (DIP-$\beta^{1-95}$) (n = 6 brains) or γ (DIP-$\gamma^{1-67}$) null mutations (n = 5 brains), respectively.

(H) Young adult (YAd; 1- to 2-day-old) DKO flies (n = 205) show enhanced tracking of a rotating optomotor stimuli compared to control flies (n = 218). Adult flies (Ad; 13–15 days) showed no difference between DKO (n = 163) and control (CTL; n = 233) flies.

(I) Young adult (YAd; 1- to 2-day-old) DKO flies (n = 105) show an enhanced preference toward the lit arm of a phototactic choice y-maze compared to control flies (n = 198). Adult flies (Ad; 13-15 days) showed no difference between DKO (n = 168) and CTL (n = 232) flies.

(J–L) ERG responses of 1- to 2-day-old DKO (n = 9) and control (n = 7) flies by intensity for the On transient (J), steady-state response (K), and Off transient (L) components of the ERG in response to a 0.6-s flash of light (see Figure S1F). Bars indicate statistical significance at the indicated intensities. Plots indicate mean of all measurements, and shaded areas indicate the SEM.

(M–N′) Confocal images (longitudinal plane of the lamina cartridges) showing the distribution of Brp (green, smFPV5) expressed in L cells (magenta, LexAop-myr-tdTOM) in the laminas of wild-type or DKO flies. Scale bars, 10 μm. White dotted lines indicate the lamina neuropil. The yellow lines show the boundary between

*(legend continued on next page)*

assembly of neural circuits in different regions of the *Drosophila* nervous system. DIP-γ and Dpr11 regulate the morphogenesis of synaptic terminals at the neuromuscular junction and regulate cell survival in the visual system (Carrillo et al., 2015; Xu et al., 2018); interactions between synaptic partners mediated by DIP-α and Dprs 6 and 10 have also been shown to regulate cell survival, control layer innervation, and synapse number and distribution in the visual system (Xu et al., 2018); binding between DIP-α and Dpr10 has further been shown to regulate terminal branching of motor neuron axons onto specific body wall and leg muscles, a process proposed to mediate synaptic specificity between motor axons and target muscles (Ashley et al., 2018; Venkatasubramanian et al., 2019); and multiple Dpr-DIP interactions are thought to mediate axon-axon fasciculation in the olfactory system (Barish et al., 2018). However, whether Dpr and DIP proteins act instructively to regulate synaptic specificity remains unclear.

To test the latter possibility, we have focused on the lamina of the *Drosophila* optic lobe (Figures 1A–1C), which comprises a highly stereotyped cellular and synaptic architecture that has been extensively characterized in electron microscopy (EM) studies (Meinertzhagen and O'Neil, 1991; Rivera-Alba et al., 2011). Within the lamina, the synaptic terminals of photoreceptors R1–R6 (R cells) and the neurites of lamina neurons L1–L5 (L cells) organize into cylindrical modules called cartridges (Figures 1A and 1B). Each cartridge receives input from R cells that detect light from the same point in visual space (Braitenberg, 1967; Kirschfeld, 1967), neighboring cartridges processing information from neighboring points in visual space so as to establish a retinotopic map in the lamina. The core of each cartridge primarily comprises the main axons of L1 and L2 and their dendrites, which are sandwiched in between a ring of six R-cell axon terminals (Figure 1B). By contrast, the main neurites of L3–L5 are located around the cartridge circumference, although L3 sends dendrites into the cartridge core. R cells repeatedly synapse *en passant* onto L1–L3 dendrites throughout each cartridge, but L1–L3 neither synapse reciprocally onto R cells nor synapse with each other (Figure 1C). In the proximal lamina, near the base of each cartridge, L4 extends dendrites into the cores of both its own cartridge (Figure 1A) and those of two neighbors and forms reciprocal connections with L2 (Figure 1C). All L cells send axons into the underlying medulla neuropil, where they synapse onto specific target cells.

Previous studies have characterized the mechanisms underlying targeting and positioning of neural processes to and within cartridges, respectively. Interactions between R cell axons (Clandinin and Zipursky, 2000; Langen et al., 2015), mediated by the cell-surface molecules N-cadherin (CadN) (Lee et al., 2001; Schwabe et al., 2013) and Flamingo (Chen and Clandinin, 2008; Lee et al., 2003; Schwabe et al., 2013), and CadN-dependent interactions between R cell axons and L cells (Prakash et al., 2005) target the axons of R cells that "view" the same point in visual space to the same cartridge. The receptor tyrosine phosphatases Lar (Clandinin et al., 2001) and PTP69D (Newsome et al., 2000) and the scaffold protein Liprin-α (Choe et al., 2006) are also required for R cell axon target specificity. Within cartridges, differential adhesion mediated by CadN optimally positions R cell and L cell neurites for synapse formation, with those cells forming the most connections (L1 and L2) occupying the cartridge core and cells forming fewer connections restricted to the periphery (Schwabe et al., 2014). In CadN mutant flies, there was a drastic reduction of R cell synapses (Schwabe et al., 2014), indicating that neurite positioning within cartridges or CadN plays a crucial role in synaptogenesis or maintenance of synapses. Despite these advances, the mechanisms that control synaptic specificity within cartridges remain unknown.

Using loss- and gain-of-function genetic approaches, we have exploited the cell-type specificity of synapse formation within lamina cartridges to ask whether DIP proteins are necessary and sufficient for synaptic specificity. Our findings demonstrate that DIP proteins are necessary for proper visual function and support a role for DIP-β in promoting synapses to form between L4 and L2 neurons. When DIP-β function is disrupted, L4 neurons form ectopic synapses. This suggests that L4 neurons have the capacity to synapse with multiple cell types, but a preference for L2 neurons is established by DIP-β, most likely through interactions with Dpr proteins. Our findings argue against the idea that specific interactions between correct synaptic partners are necessary for synapse formation and support a model whereby instead, such interactions establish a relative preference for synapses to form between specific cell types.

## RESULTS

### DIP Proteins Are Necessary for Proper Synaptic Connectivity and Visual Function

In the lamina, L4 and L2 neurons selectively form reciprocal connections in the proximal lamina (Meinertzhagen and O'Neil, 1991; Rivera-Alba et al., 2011). L2 abuts L1 extensively throughout the cartridge (Figure 1B) yet is only presynaptic in the proximal region, where it synapses primarily onto L4, while L4 dendrites extend into the proximal cartridge core (Figure 1A) and encounter both L1 and L2 neurites yet primarily synapse onto L2. A previous study demonstrated that during synaptogenesis, L4 dendritic branches strongly express the IgSF protein Kirre, and that disrupting *kirre* reduces the number of L4-L2 synapses (Lüthy et al., 2014). Thus, Kirre is required for synapse formation or maintenance in this context. However, the mechanisms underlying the selectivity of synapse formation between L4 and L2 neurons remain unknown. Previously, through use of

the distal and proximal lamina. (M and M′) In wild-type flies (n = 9 brains), Brp is restricted to the proximal lamina, where L2 and L4 neurons are known to form synapses. (N and N′) In DKO flies (n = 7 brains), Brp is still localized to the proximal lamina, but ectopic Brp puncta are present in the distal lamina.
(O–Q) Average number of Brp puncta in the distal (O) or proximal (P) halves of lamina cartridges from different genotypes, and average total number of Brp puncta within lamina cartridges (Q). Results are from two different experiments (1 or 2). Statistical significance was established with respect to wild-type flies (see STAR Methods for a detailed description of statistical analyses). Data are presented as mean ± SEM.
(R) Shows the number of distal Brp puncta within individual cartridges scored in wild-type and DKO flies. Each star indicates a cartridge; ±SEM is shown in red. Statistical significance: *p < 0.05, **p < 0.005, ***p < 0.0005. See also Figure S1.

RNA sequencing (RNA-seq) and GAL4 reporters, both L4 and L2 were found to express a single DIP during pupal development, with L4 expressing DIP-β and L2 expressing DIP-γ (Tan et al., 2015). DIP-β is known to bind to seven different Dpr proteins *in vitro* (Carrillo et al., 2015; Cosmanescu et al., 2018; Özkan et al., 2013), six of which have been shown to be expressed in L2 neurons (Tan et al., 2015). DIP-γ is known to bind 4 Dprs *in vitro* (Özkan et al., 2013). While L4 was not found to express any of these Dprs at 40 h after puparium formation (APF) (Tan et al., 2015), we reasoned that L4 may express one or more of these during actual synapse formation, which occurs later in development (see below). Thus, we hypothesized that DIP-β-Dpr interactions, DIP-γ-Dpr interactions, or both promote selective synapse formation between L4 and L2 neurons. As DIPs-β and γ bind to many Dprs, to test this hypothesis, we concentrated our efforts on addressing the functions of DIPs-β and γ.

Using the CRISPR/Cas9 system, we generated early stop mutations near the translational start sites of DIPs-β and γ (see STAR Methods). DIP-β and γ immunolabeling were as a result eliminated in the optic lobes of flies homozygous for these mutations (Figures 1D–1G), demonstrating their effectiveness in disrupting DIP function. To determine if DIPs-β and γ are important for circuit formation in the visual system, we assessed whether disrupting these genes in combination (i.e., double knockout [DKO]) caused deficits in visual function using behavioral and physiological assays (Werkhoven et al., 2019). We found that young adult (YAd) 1- to 2-day-old DKO flies were more responsive to apparent motion cues compared with control flies in the optomotor assay (Figure 1H) and showed a stronger photopositive bias than control flies in the phototaxis assay (Figure 1I). Interestingly, these effects were transient, because adult (Ad) 13- to 15-day-old DKO and control flies performed similarly in both assays (Figures 1H and 1I). In the phototaxis assay, we also observed differences in the average speed between adult DKO and control flies and the number of trials triggered by both young adult and adult DKO and control flies, likely due to differences in activity (Figures S1B and S1C). Our data indicate that DIP-β, γ, or both are required for visually guided behavior. Electroretinogram (ERG) recordings revealed significant differences between DKO and control flies for both On and Off transient responses, which are thought to correspond to the activities of L1 and L2 neurons (Coombe, 1986), and for the sustained component (SS) corresponding to the photoreceptor response (Heisenberg, 1971) (Figures 1J–1L and S1F). These differences varied as a function of light intensity and were most pronounced at intermediate light intensities (Figures 1J–1L). The phototactic bias was similarly largest at intermediate light intensities (Figures S1D and S1E), suggesting that abnormal phototaxis in DKO flies might be caused by altered neural activity in the visual system. Taken together, these findings demonstrate that DIP-β, γ, or both are necessary for proper visual function, motivating further investigation of their potential role in regulating connectivity between L4 and L2 neurons.

To test whether DIP proteins are necessary for synaptic specificity, we used synaptic tagging with recombination (STaR) (Chen et al., 2014; Peng et al., 2018) to label L4-L2 synapses selectively. Using STaR, the active zone protein Bruchpilot (Brp) (Wagh et al., 2006) can be tagged in a cell-type-specific manner depending on the expression of FLP recombinase (Golic and Lindquist, 1989) while being expressed from its native promoter within a bacterial artificial chromosome (BAC). Moreover, the cells that express tagged Brp can also be made to express a fluorescent reporter through the LexA/LexAop system (Lai and Lee, 2006), providing a context in which to assess Brp localization. It has been shown that Brp puncta number correlates well with synapse number determined by EM (Chen et al., 2014). Since L4 and L2 are the only L cells that are presynaptic in the lamina and because they predominantly synapse with each other (Meinertzhagen and O'Neil, 1991; Rivera-Alba et al., 2011), selectively expressing FLP in L cells allows selective visualization of L4-L2 synapses in the proximal lamina (Figures 1M, 1M′, and S1A). In the absence of DIP function, we expected to observe a reduction in the number of Brp puncta in the proximal lamina, which would indicate a loss of L4-L2 synapses. However, in flies doubly mutant for DIPs-β and γ (DKO flies), the number of Brp puncta in the proximal lamina was qualitatively similar to that of wild-type flies (Figure 1N and 1N′). Interestingly, we observed abnormally large numbers of Brp puncta in the distal lamina of DKO flies compared with wild-type flies, indicating that in the absence of DIP function, additional synapses form at ectopic locations.

To quantify this phenotype, we imaged along the long axis of lamina cartridges using confocal microscopy and took z stacks of the laminas of wild-type and DKO flies. Using a customized machine-learning algorithm (see STAR Methods), we segmented individual cartridges and counted the number of Brp puncta within distal and proximal halves. As the proximal lamina in wild-type flies, defined by the location of L4 dendrites and L4-L2 synapses, spans less than half of the lamina neuropil, the number of distal lamina synapses counted with this method may represent an underestimate. We found that the average number of Brp puncta in the distal halves of cartridges was significantly higher in DKO flies than in wild-type flies (Figures 1O and 1R). A statistically significant difference in the number of Brp puncta in the proximal halves of cartridges from DKO flies relative to wild-type flies was not observed (Figure 1Q), but many synapses form in this region compared to the distal lamina. Additionally, no difference in the total number of Brp puncta within cartridges from DKO versus wild-type flies was detected. Thus, in DKO flies, L cell synapses still form in the lamina, but some are abnormally distributed within the distal lamina. Together, these data indicate that DIP proteins are necessary for proper synaptic connectivity but are not required for synapse formation.

## L4 Neurons Form Ectopic Synapses and Have Altered Dendrite Morphology in the Absence of DIP-β Function

To assess which L cell subtypes contribute ectopic Brp puncta in the distal lamina in the absence of DIP function, we used STaR to selectively label Brp in each L cell independently in wild-type, control (β+/−; γ+/−), or DKO flies using cell-type-specific GAL4 drivers (Tuthill et al., 2013) to control expression of FLP recombinase. These experiments revealed that L4 neurons (Figures 2A–2C) have an increased number of Brp puncta in the distal laminas of DKO flies compared with wild-type flies (Figure 2D). We did not observe differences in the number of Brp puncta in the proximal lamina or the total number of puncta

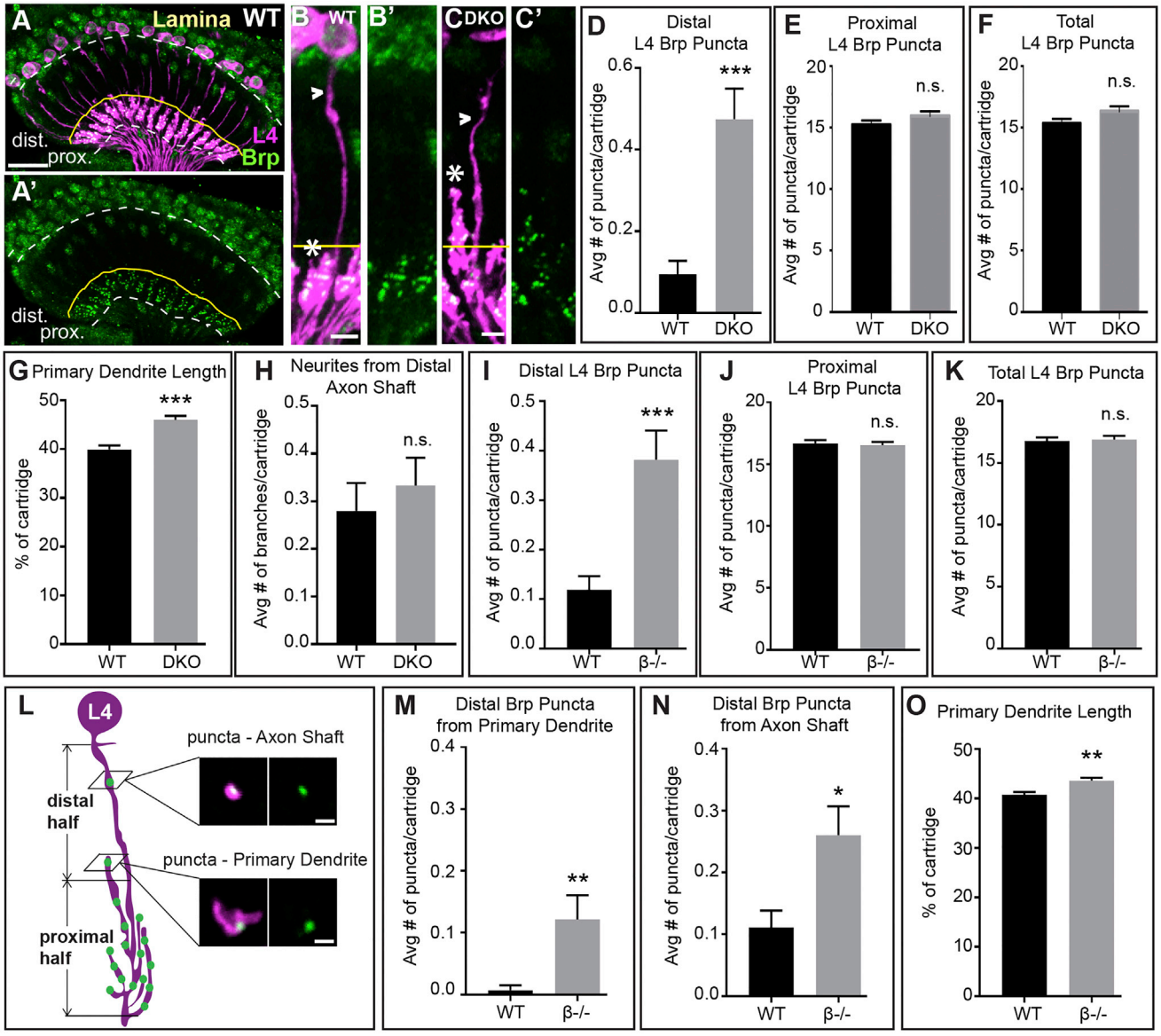


**Figure 2. L4 Neurons Form Ectopic Synapses and Have Altered Dendrite Morphology in the Absence of DIP-β Function**

(A and A′) Confocal images (longitudinal plane of the lamina cartridges) showing the distribution of Brp (green, smGFPV5) expressed in L4 cells (magenta, LexAop-myr-tdTOM, 31C06AD (II), 34G07DBD (III) L4 split-GAL4 + UAS-FLP) in the lamina of wild-type flies. Brp is restricted to the proximal lamina, where L4 neurons are known to form synapses (n = 7 brains). White dotted lines indicate the lamina neuropil. The yellow lines show the boundary between the distal and proximal lamina. Scale bar, 10 μm.

(B–C′) Confocal images of L4 neurons expressing Brp-smGFPV5 (STaR) in wild-type (B and B′) and DKO flies (C and C′). In DKO flies primary dendrites extend into the distal lamina. Arrowheads indicate L4 axons and asterisks indicate primary dendrites. The yellow line approximates the boundary between the proximal and distal lamina. Scale bars, 5 μm.

(D–F) The average number of Brp puncta in L4 neurons present within the distal (D) or proximal (E) halves of lamina cartridges, and the average total number of puncta within cartridges (F) in wild-type or DKO flies (distal: wild-type, n = 105 cartridges, 7 brains; DKO, n = 120 cartridges, 8 brains; proximal and total: wild-type, n = 75, 5 brains; DKO n = 75 cartridges, 5 brains). Data are presented as mean ± SEM.

(G) L4 primary dendrite length calculated as percentage of total cartridge length in wild-type (n = 105 cartridges) and DKO (n = 120 cartridges) flies.

(H) Average number of neurites protruding from L4 axons in the distal half of the lamina in wild-type (n = 75 cartridges) and DKO (n = 75 cartridges) flies. Data are represented as a mean ± SEM.

(I–K) The average number of Brp puncta in L4 neurons present within the distal (I) or proximal (J) halves of lamina cartridges, and the average total number of puncta within cartridges (K) in wild-type or in DIP-β KO flies (wild-type n = 135 cartridges; 9 brains, DIP-β KO n = 165 cartridges; 11 brains). Data are presented as mean ± SEM.

*(legend continued on next page)*

per cartridge (Figures 2E and 2F). The increase in distal Brp puncta in L4 neurons is less than that observed when visualizing Brp in all L cells (compare Figures 1O and 2D), indicating that other L cells may contribute to the phenotype. However, in the distal halves of the laminas of DKO flies, increased numbers of Brp puncta were not detected in L1–L3 or L5 neurons (Figures S2A–S2K) compared with control or wild-type flies. As the GAL4 drivers for L1–L3 and L5 neurons turn on in the adult stage, it remains possible that limited expression of tagged-Brp in these neurons was insufficient to label all their presynaptic sites. By contrast, in experiments where Brp was labeled in L4 or all L cells, tagged Brp is activated in early pupal development or from the time the L cells are born, respectively.

In DKO flies, L4 axons were morphologically indistinguishable from L4 axons in wild-type flies (Figures 2B, 2C, and 2H). However, the primary dendrites of L4 neurons in DKO flies extended more distally within the cartridge core than did primary dendrites from wild-type flies (Figures 2B, 2C, and 2G), even though the general spacing of primary L4 dendrites appeared normal (Figures S2L and S2M).

To determine whether the synaptic and dendritic phenotypes in DKO flies resulted from disrupting DIP-β, γ, or both, we analyzed single KO flies. We found that disrupting one or both copies of DIP-β caused an increase in the number of Brp puncta in L cells in the distal lamina similar to DKO flies (Figure 1O) and an increase in the total number of Brp puncta per cartridge (Figure 1Q). Disrupting one copy of DIP-β considerably reduced DIP-β immunolabeling in the optic lobe (Figures S1G and S1H). When both copies of DIP-β were disrupted, we also observed a significant increase in the number of Brp puncta L cells form in the proximal lamina (Figure 1P). Cell-type-specific STaR experiments revealed that, as in DKO flies, in DIP-β KO flies, L4 neurons have increased numbers of Brp puncta in the distal lamina compared with wild-type flies (Figure 2I). In addition, primary dendrites extended further distally in DIP-β KO flies than in wild-type flies (Figure 2O), similar to what we observed in DKO flies (Figure 2G). In DIP-β KO flies, the majority of distal Brp puncta were present on L4 axon shafts, with only a subset formed on primary dendrites (Figures 2L–2N). Thus, ectopic synapse formation in the distal lamina under these conditions does not correlate with altered dendritic morphology. KO of DIP-γ did not result in a statistically significant difference in distal or proximal Brp puncta relative to wild-type flies (Figures 1O and 1P). Collectively, these findings indicate that disrupting DIP-β causes L4 neurons to form ectopic synapses and have altered dendritic morphology.

## DIP-β Is Cell-Autonomously Required in L4 Neurons for Proper Synaptic Connectivity

DIP-β is expressed in multiple cell types in the visual system (Cosmanescu et al., 2018) (Figure 1D), and so to determine if synaptic defects observed in DIP-β KO flies result from the disruption of DIP-β in L4 neurons as opposed to other neurons, we undertook conditional knockdown (cKD) experiments. We expressed DIP-β RNAi exclusively in L cells and visualized L cell synapses in the lamina using STaR. As DIP-β is normally expressed in L4 but no other L cells (Tan et al., 2015), disrupting DIP-β in all L cells is analogous to disrupting DIP-β in L4 neurons alone. Developmental analyses revealed that DIP-β immunolabeling becomes detectable in the proximal lamina in a pattern reminiscent of L4 dendritic processes at 72 h APF (Figures S3A–S3C′), and this labeling is eliminated in DIP-β KO flies (Figures 3A and 3B). Expressing DIP-β RNAi in L cells (Figures 3C–3D′) or L4 neurons selectively (Figures S3C–S3D″) also significantly reduced DIP-β immunolabeling in the proximal lamina, demonstrating the efficacy of knockdown and showing that L4 dendrites are the primary source of DIP-β in this region. Additionally, when DIP-β was knocked down in L cells, we observed increases in Brp puncta in the distal (Figures 3E and 3G) and proximal (Figure 3F) lamina similar to that observed in whole-fly DIP-β mutants (Figures 1O and 1P). These findings demonstrate that DIP-β is required in L4 neurons to establish normal synaptic connectivity.

## DIP-β Localizes to L4 Dendrites during Synapse Formation

To gain further insight into DIP-β function, we assessed the timing of DIP-β expression in L4 neurons with respect to the formation of L4-L2 synapses and its subcellular localization during synapse formation visualized through immunolabeling and confocal microscopy. DIP-β immunolabeling was not detected in the lamina at 24 h APF (Figure S3A), but strong immunolabeling was detected in the most distal region of the lamina neuropil at 48 h APF (Figure S3B). This labeling likely represents DIP-β expressed in LaWF2 neurons (Tuthill et al., 2013). At 72 h APF, faint immunolabeling could be observed in the proximal lamina on L4 dendrites (Figures 3A–3D′ and S3C–S3D″). To determine if the timing of DIP-β localization to L4 dendrites coincided with synapse formation, we used STaR to label Brp in L cells (Figure S1A) and assessed Brp localization during pupal development in the laminas of wild-type flies. We found that L4-L2 synapses form between 46 and 69 h APF (Figures 3H–3I′), similar to the time when DIP-β becomes localized to L4 dendrites (between 48 and 72 h APF) (Figures 3A, 3C, and S3A–S3C′). To shed light on whether DIP-β localizes to developing synapses, we simultaneously visualized DIP-β (immunolabeling) and Brp in L cells (STaR) at 72 h APF using confocal microscopy (Figures 3J–3J″). We found that DIP-β was more diffusely distributed than Brp but that some of the DIP-β protein appeared to be organized into clusters that overlapped with or were adjacent to Brp puncta. This was consistent between cartridges and across

(L) Illustration of L4 morphology and presynaptic sites (Brp puncta) in the lamina of a DIP-β KO fly. Primary dendrites are mostly located in the proximal half of the lamina, with some extending into the distal half. Brp puncta are observed in the distal half from two sources, the axon shaft and primary dendrites. Scale bars, 1 μm.

(M and N) The average number of distal Brp puncta from L4 primary dendrites (M) or L4 axon shafts (N) in wild-type (n = 135 cartridges) and DIP-β KO (n = 165 cartridges) flies.

(O) L4 primary dendrite length calculated as percentage of total cartridge length in wild-type (n = 135 cartridges) and DIP-β KO (n = 165 cartridges) flies.

Statistical significance: *p < 0.05, **p < 0.005, ***p < 0.0005. See also Figure S2.

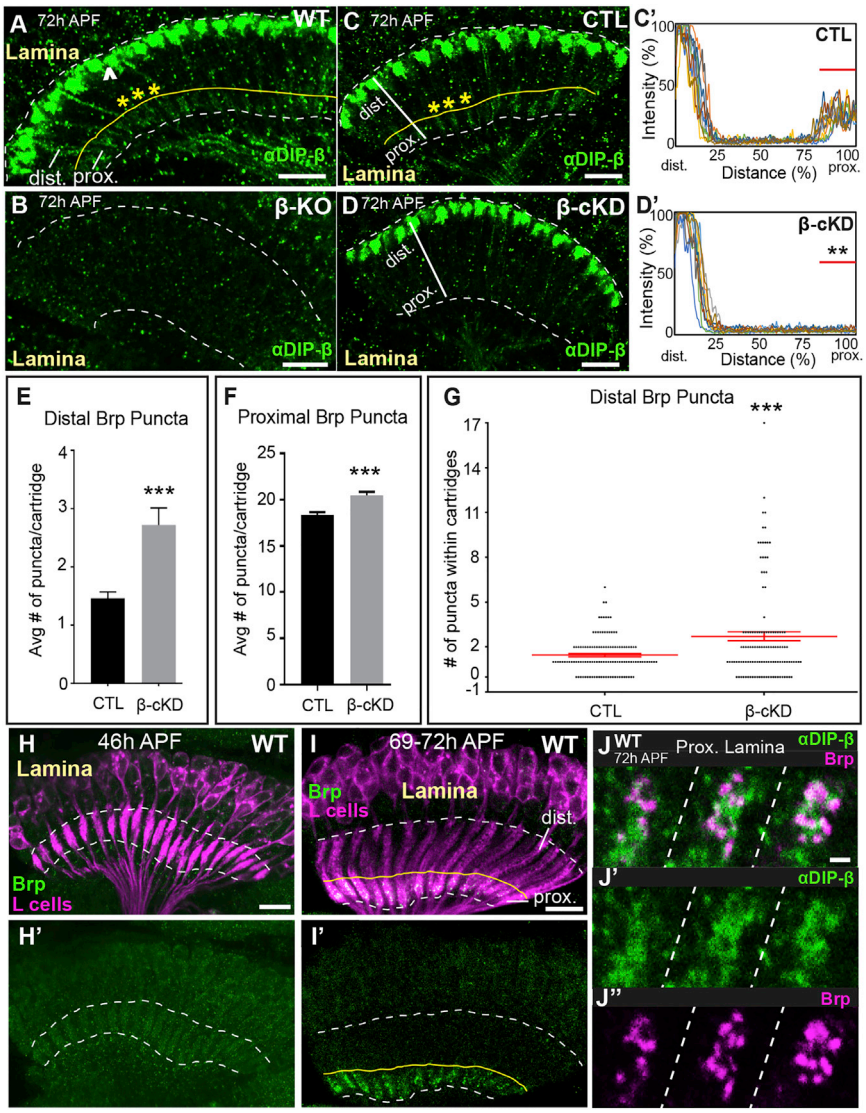


**Figure 3. DIP-β in L4 Neurons Is Necessary for Proper Synaptic Connectivity**

(A and B) Confocal images showing DIP-β immunolabeling (green) in the laminas of wild-type (A) or DIP-β KO flies (B) at 72h APF. The dotted white lines demarcate the lamina neuropil. The yellow line in (A) indicates the boundary between the proximal and distal lamina. The arrowhead in (A) indicates DIP-β expression in non-L4 neurons likely to be LaWF2 neurons. Yellow asterisks in (A) indicate individual cartridges. Scale bars, 10 μm.

(C–D′) DIP-β immunolabeling in the proximal lamina at 72 h APF in control (UAS-β-RNAi only) and conditional knockdown flies (β-cKD; UAS-β-RNAi + 9B08-GAL4). (C and D) Confocal images of DIP-β immunolabeling in the laminas of a control fly (C) or a β-cKD fly (D). The white lines show the region of lamina cartridges assessed in (C′ and D′). In (C), the yellow asterisks indicate individual cartridges. Scale bars, 10 μm. (C′ and D′) Quantification of DIP-β fluorescence intensity along the long axis of lamina cartridges (see white lines in C and D). Significantly reduced fluorescence intensity is observed in the proximal lamina (80%–100% distance) of β-cKD flies (the proximal lamina is marked by red bar in C′ and D′) compared to control flies (n = 3 cartridges per brain, n = 10 brains per condition).

(E) The average number of Brp puncta in the distal halves of lamina cartridges in control (n = 120 cartridges; 6 brains) and β-cKD (n = 120 cartridges; 6 brains) flies. Data are presented as mean ± SEM.

(F) The average number of Brp puncta in the proximal halves of lamina cartridges in control (n = 120 cartridges; 6 brains) and β-cKD (n = 120 cartridges; 6 brains) flies. Data are presented as mean ± SEM.

(G) Total number of Brp puncta in the distal halves of cartridges in control (n = 120 cartridges; 6 brains) and β-cKD (n = 120 cartridges; 6 brains) flies. Each dot represents a cartridge. Red bar indicates ±SEM.

(H–I′) Confocal images in a longitudinal plane of lamina cartridges showing the developmental timing of Brp expression (green, smGFPV5) in L cells (magenta, myr-tdTOM) in the lamina. The dotted lines delineate the lamina neuropil. The yellow line in (I) and (I′) indicates the boundary between the distal and proximal lamina. n = 5 brains (46 and 69–72 h APF for H–I′). Scale bars, 10 μm.

(J–J″) Co-labeling of DIP-β (green) and Brp (magenta- smGFPV5) at 72h APF in the proximal regions of three lamina cartridges separated by dotted lines. Scale bars, 1 μm.

Statistical significance: *p < 0.05, **p < 0.005, ***p < 0.0005. See also Figure S3.

brains. Taken together, these findings show that DIP-β localizes to L4 dendrites during synapse formation between L4 and L2 neurons, consistent with a role for DIP-β in establishing connectivity between these neurons.

## DIP Mis-expression Promotes Synapse Formation in Dpr-Expressing Lamina Neurons

If Dpr-DIP interactions act instructively to control synaptic specificity, then they should be sufficient to promote synapse formation between specific cell types. To test this possibility, we exploited the cell-type specificity of synaptic connections between L cells and R cells in the lamina. Within each cartridge, R cells synapse *en passant* onto L1–L3, but L1–L3 do not reciprocally synapse back onto R cells, nor do they synapse with each other (Meinertzhagen and O'Neil, 1991; Rivera-Alba et al., 2011) (Figure 1C). This specificity is striking given that processes of these neurons are densely packed within the cartridge and contact each other extensively. L cells express high levels of Dprs (Tan et al., 2015), and in general, both L cells and R cells express low levels of DIPs (Tan et al., 2015; Zhang et al., 2016). Thus, we hypothesized that if Dpr-DIP interactions promote synapse formation, then mis-expressing DIPs in R cells should cause L cells to synapse onto R cells. Likewise, mis-expressing DIPs in L1–L3 should cause these cells to synapse with each other.

To test this hypothesis, we mis-expressed DIPs-γ and ε either together or independently and DIP-β independently in R cells or

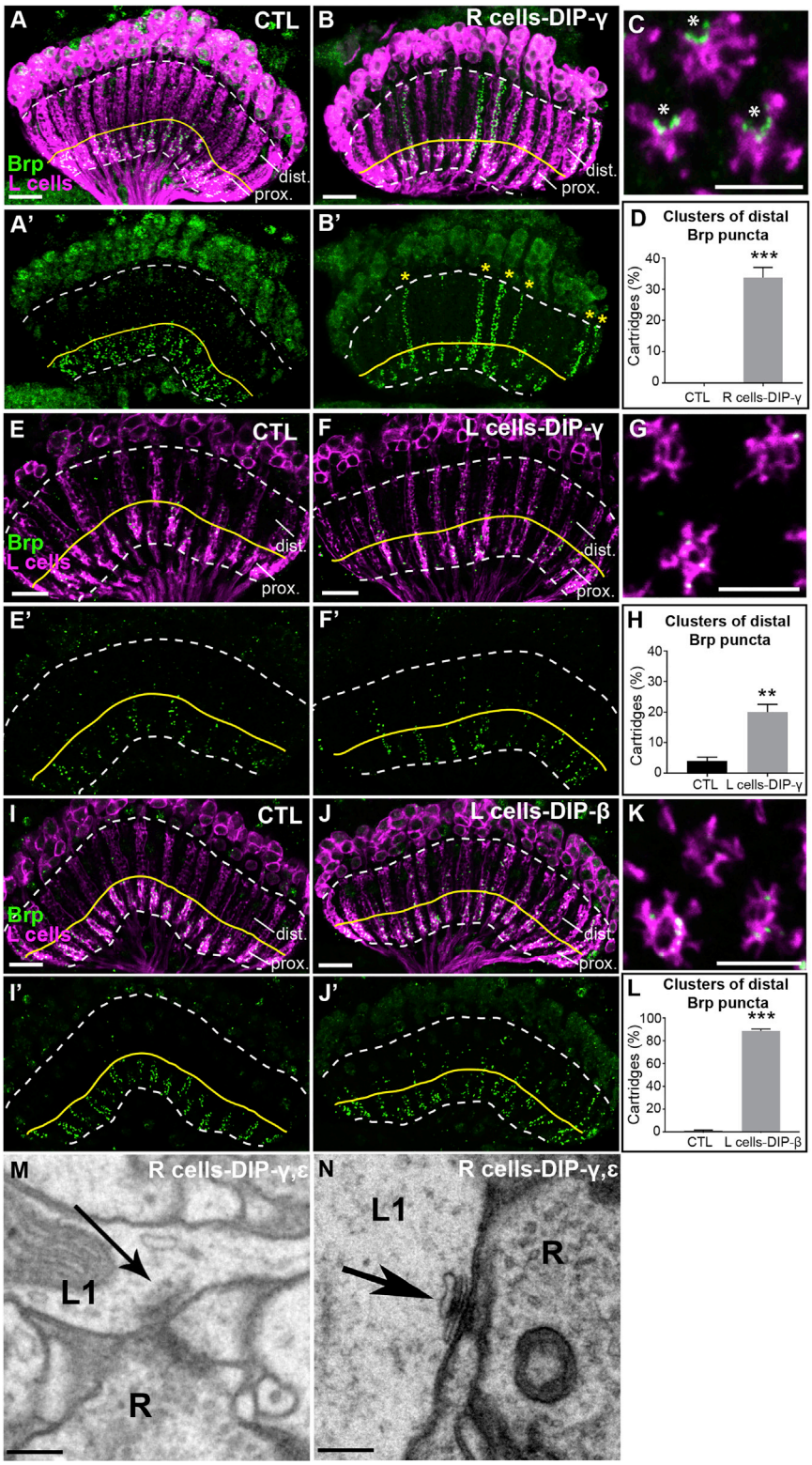


**Figure 4. DIP Mis-expression Promotes Synapse Formation with Dpr-Expressing Lamina Neurons**

(A–B′) Confocal images (longitudinal plane of lamina cartridges, 1- to 2-day-old adults) showing the distribution of Brp (green, smFPV5) expressed in L cells (magenta, LexAop-myr-tdTOM) in the laminas of control (UAS-DIP-γ) flies or flies expressing DIP-γ in R cells (UAS-DIP-γ and GMR-GAL4). The white dotted line outlines the lamina, and the yellow line separates the proximal (prox.) and distal lamina (dist.). Scale bars, 10 μm. (A and A′) Brp is restricted to the proximal lamina in control flies. (B and B′) Streams of ectopic Brp puncta are detected throughout lamina cartridges (yellow stars in B′) when mis-expressing DIP-γ in R cells.

(C) A confocal image of a cross section through the lamina of a fly mis-expressing DIP-γ in R cells. Asterisks indicate the presumed positions of photoreceptor axons. Scale bar, 5 μm.

(D) Quantification of the percentage of cartridges containing clusters of Brp puncta in the distal lamina in control flies (n = 11) and flies mis-expressing DIP-γ in R cells (n = 11). Clusters were defined as three or more consecutive z stack slices containing distal Brp puncta. Only unmerged cartridges were considered in the quantification (n = 25 cartridges/brain). Data are presented as mean ± SEM.

(E–F′) Mis-expression of DIP-γ in L cells (27G05-GAL4). Confocal images show the distribution of Brp (green, smFPV5) expressed in L cells (magenta, LexAop-myr-tdTOM) in the laminas of control flies (27G05-GAL4 alone) or experimental flies (27G05-GAL4 and UAS- DIP-γ). The region above the yellow line delineates the distal lamina (dist.). Scale bars, 10 μm. (E and E′) Brp is localized to the proximal lamina in control (27G05-GAL4) flies, occasionally with some puncta in the distal lamina (n = 5 brains). (F and F′) L cells form ectopic synapses in the distal regions of lamina cartridges upon mis-expression of DIP-γ in L cells (n = 5 brains).

(G) A confocal image of a cross section through the lamina of a fly mis-expressing DIP-γ in L cells. Scale bar, 5 μm.

(H) Quantification of percentage of cartridges containing clusters of Brp puncta in the distal lamina in control flies (n = 5) and flies mis-expressing DIP-γ in L cells (n = 5). Clusters were defined as five or more distal Brp puncta within five consecutive z stack slices of each cartridge (n = 25 cartridges/brain). Data are presented as mean ± SEM.

(I and I′) Brp is localized to the proximal lamina in control (UAS-DIP-β) flies (n = 5 brains).

(J and J′) In flies mis-expressing DIP-β in L cells (27G05-GAL4), ectopic synapses are present throughout lamina cartridges (n = 7 brains).

(K) A confocal image of a cross section through the lamina of a fly mis-expressing DIP- β in L cells. Scale bar, 5 μm.

(L) Quantification of percentage of cartridges containing clusters of Brp puncta in the distal lamina in control flies (n = 5) and flies mis-expressing DIP-β in L cells (n = 5). Clusters were defined as five or more distal Brp puncta within five consecutive z stack slices of each cartridge (n = 25 cartridges/brain). Data are presented as mean ± SEM.

*(legend continued on next page)*

L cells and visualized L cell synapses in the lamina using STaR as in the DIP KO experiments. We chose these DIPs because they have broad Dpr-binding specificities and are known to bind to Dprs expressed in L cells (Carrillo et al., 2015; Cosmanescu et al., 2018; Özkan et al., 2013; Tan et al., 2015). In control flies, L cell synapses were restricted to the proximal lamina, where L4 and L2 form reciprocal connections (Figures 4A and 4A′). Strikingly, mis-expression of both DIPs-γ and ε (Figures S4A and S4A′) or DIP-γ alone in R cells (Figures 4B and 4B′) caused L cells to form streams of ectopic synapses throughout lamina cartridges. On average, 34% of lamina cartridges in young adult (1- to 2-day-old) flies mis-expressing DIP-γ in R cells displayed clusters of ectopic L cell synapses in the distal lamina, while none of the cartridges in control flies showed this phenotype (Figure 4D). While both DIPs-ε and γ were strongly expressed upon mis-expression in R cells (Figures S4C and S4D), mis-expression of DIP-ε alone did not cause the formation of ectopic synapses (Figures S4B and S4B′), nor did mis-expression of DIP-β (Figures S4G and S4G′).

Cross sections through the lamina of flies mis-expressing DIP-γ in R cells revealed the presence of fused cartridges in both control and mis-expression flies (Figures S4E and S4F). The presence of the GMR-GAL4 driver alone (R cell expression) was sufficient to induce cartridge fusion (Figure S4E). Importantly, the induction of ectopic synapses does not correlate with cartridge fusion, as many unfused cartridges contained ectopic synapses (Figures 4C, 4D, and S4F). Analysis of cross sections also revealed that ectopic synapses frequently formed on the edges of L cell profiles consistent with the positions of R cell axon terminals (Figure 4C).

Mis-expression of DIPs-γ (Figures 4E–4H) or β (Figures 4I–4L) only in L cells also caused L cells to form ectopic synapses throughout lamina cartridges. Mis-expression of DIP-γ in L cells induced ectopic synapse formation in ~20% of lamina cartridges (Figure 4H), while ~90% of cartridges contained clusters of Brp puncta in the distal lamina upon DIP-β mis-expression in L cells (Figure 4L). Cross section views through cartridges revealed that ectopic Brp puncta were distributed throughout L cell processes within cartridges (as opposed to the edges of cartridges as in R cell mis-expression experiments) (compare Figures 4C, 4G, and 4K), consistent with L cell-L cell synapses.

Together, these findings show that mis-expression of DIPs-γ and β causes L cells to form ectopic synapses in a predictable manner. To visualize the morphologies and cellular constitution of ectopic synapses induced by DIP mis-expression, we utilized EM. We cut the lamina of a fly mis-expressing both DIPs-γ and ε in R cells into 50- to 60-nm sections and imaged these using transmission electron microscopy (TEM). We then identified the synapses formed in the sections and assigned them to cellular profiles based on previously established criteria (Meinertzhagen, 1996; Meinertzhagen and O'Neil, 1991). We found that the positions of cell types within the cartridge were normal, with L1 and L2 always paired at the cartridge axis surrounded by R cell terminals (Figure S5). In addition, the numbers of synapses formed by R cells (R cells presynaptic) was similar to those reported previously for the wild-type, with the 6 R cell profiles together contributing 330 synapses (Table S1) (Meinertzhagen and O'Neil, 1991; Rivera-Alba et al., 2011). Thus, DIP-mis-expression did not significantly perturb the general cellular architecture of the cartridge, or synapse formation in R cells. We identified 86 L cell synapses within the cartridge (L cells presynaptic) (Table S1), which are approximately three or four times more L cell synapses than was previously reported for wild-type cartridges (Meinertzhagen and O'Neil, 1991; Rivera-Alba et al., 2011). These were distributed throughout the cartridge, with 31 L cell synapses in the distal half (Table S1). In addition, we identified presynaptic sites formed by L1 (×12), L3 (×13), and L5 (×5) neurons that were previously not found to be presynaptic in the lamina (we also identified L2 and L4 presynaptic sites). In some cases, identified R cell profiles were adjacent to L cell presynaptic sites (Figures 4M and 4N), consistent with L cell to R cell synapses, although a full reconstruction would be necessary to determine the degree to which L cell synapses form onto R cells upon DIP mis-expression. Together, these findings complement and support our confocal analyses and show that DIP mis-expression promotes synapse formation in a manner predicted by Dpr expression.

## DISCUSSION

Neurobiologists have long thought that appropriate synaptic partners express complementary molecules that allow them to identify each other within a dense meshwork of alternative neurites through a lock-and-key mechanism. A common interpretation of this idea is that interactions between correct partners mediated by complementary adhesion or recognition molecules are necessary for synaptogenesis in an "all or nothing" process. Based on their heterophilic binding and matching expression in synaptically connected cell types, Dpr and DIP IgSF proteins have been proposed to play an instructive role in regulating synaptic specificity through a complementary binding mechanism. The findings we present here support a role for DIP proteins in instructing synaptic partner selection, most likely through interactions with Dpr proteins. However, rather than being necessary for synaptogenesis, we propose that DIP proteins regulate synaptic specificity by establishing a preference for synapses to form between specific cell types (see below). In this view, synaptic specificity reflects a relative preference for certain partners rather than an absolute or categorical recognition. In the absence of such preference, neurons have the capacity to synapse with other cell types.

### DIP Proteins Are Necessary for Correct Visual Function

Our findings demonstrate that DIP-β, γ, or both are required for proper visual function. In DKO flies, we observed changes in two visually guided behaviors, the optomotor reflex and phototaxis,

(M and N) Putative L1-R cell synapses in flies mis-expressing DIPs-γ and ε in R cells identified by EM. Scale bars, 200 nm.
(M) Putative L1-R cell synapse in flies mis-expressing DIPs-γ and ε in R cells identified by EM. Scale bar, 200 nm.
(N) Putative L1-R cell synapse in flies mis-expressing DIPs-γ and ε in R cells identified by EM. Scale bar, 200 nm.
Statistical significance: *p < 0.05, **p < 0.005, ***p < 0.0005. See also Figures S4 and S5 and Table S1.

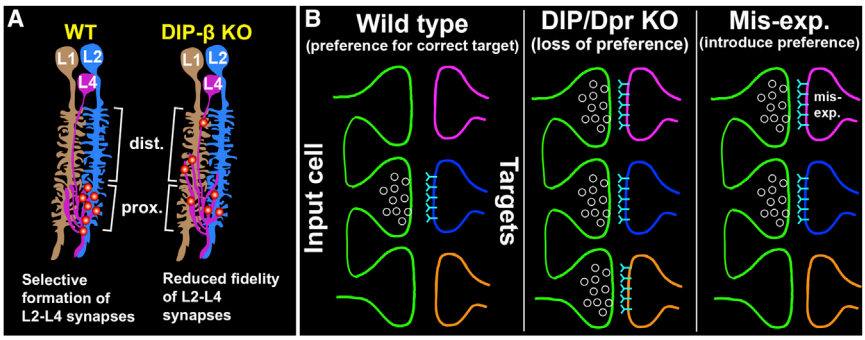


**Figure 5. Dpr-DIP Interactions May Regulate Synaptic Specificity by Establishing a Preference for Synaptic Partners**

(A) Working model of how DIP-β-Dpr interactions may regulate selective synapse formation between L4 and L2 neurons. In wild-type flies, L4 and L2 selectively synapse with each other in the proximal lamina. In DIP-β KO flies, we propose that the fidelity of L4-L2 synapse formation is reduced and that L4 neurons form synapses with alternative cell types (e.g., L1) in both the distal and proximal lamina.

(B) General model of how Dpr-DIP interactions may regulate synaptic specificity. (Left panel) In a wild-type background, Dpr-DIP interactions establish a preference for synapses to form between appropriate synaptic partners, potentially by concentrating synaptic machinery to specific cell-cell contacts. (Middle panel) When Dpr-DIP interactions are disrupted, there is a reduced preference for the correct synaptic partner. Neurons have the capacity to synapse with other cell types. (Right panel) Inducing ectopic Dpr-DIP interactions introduces a preference for inappropriate synaptic partners.

and also saw altered responses of photoreceptors and L1 and L2 neurons to light in electroretinogram recordings. For both optomotor and phototaxis assays, the phenotype in young adult DKO flies was not present in adult DKO flies. One interesting possibility is that through experience, DKO flies are able to compensate for the lack of DIP function. Whether the behavioral and physiological abnormalities observed in DKO flies are caused by the synaptic phenotypes reported here remains to be determined.

## DIP-β Is Required for Proper Synaptic Connectivity

We hypothesize that DIP-β regulates L4-L2 connectivity in multiple ways. First, DIP-β regulates the morphology of primary L4 dendrites. We hypothesize that interactions between DIP-β and L2 Dprs mediate adhesion between primary L4 dendrites and L2 processes in the cartridge core. We speculate that when this adhesion is reduced by disrupting DIP-β, L4 dendrites extend further distally and contact and synapse with alternative cell types (e.g., L1) in the distal lamina (Figure 5A). However, as most ectopic synapses form on L4 axons in DIP-β KO flies, ectopic synapse formation does not strongly correlate with altered dendritic morphology.

Second, our mis-expression experiments support a synapse promoting function for DIP-β. As mis-expression of DIP-β in L cells, but not R cells, was sufficient to induce ectopic synapse formation in L cells, DIP-β may act presynaptically to promote synapse formation. We speculate that DIP-β in L4 neurons binds to Dprs in L2 neurons and promotes synapse formation onto L2 neurons by recruiting synaptic machinery to sites of L4-L2 contact. Thus, disrupting DIP-β may result in the accumulation of synaptic proteins at sites of contact with other cell types, leading to abnormal synapse formation in the proximal and distal lamina (Figure 5A). Consistent with this, in DIP-β KO flies, most of the ectopic presynaptic sites in the distal lamina form on L4 axons, which are restricted to the cartridge periphery. It is likely that these ectopic synapses represent synapses with cell types other than L2, which occupies the cartridge core.

Our findings support a role for DIP-β in establishing L4-L2 connectivity by regulating dendrite morphology and promoting synapse formation. As DIP proteins are primarily known to bind heterophilically with Dpr proteins (Carrillo et al., 2015; Cheng et al., 2019; Cosmanescu et al., 2018; Özkan et al., 2013) (some DIPs bind homophilically; Cosmanescu et al., 2018) and disrupting DIP-Dpr interactions *in vivo* has been shown to phenocopy the loss of DIPs or Dprs (Xu et al., 2018), it is likely that DIP-β functions in both contexts by interacting with cognate Dpr proteins expressed in L2 neurons. However, we cannot rule out Dpr-independent functions. To test this, it is crucial to identify Dprs expressed in L2 that bind DIP-β during synapse formation and test whether disrupting them, or the ability of DIP-β to bind them, phenocopies the loss of DIP-β in L4 neurons. We previously showed that L2 neurons express six of the seven Dprs known to bind DIP-β at 40 h APF and at least two of these Dprs at 72 h APF (Tan et al., 2015) (Table 1). L1 neurons were found to express three of the seven Dprs at 40 h APF and at least one of these Dprs at 72 h APF (Tan et al., 2015) (Table 1). Thus, the preference for L4 neurons to synapse with L2 neurons over L1 neurons may be accounted for by the fact that L2 neurons express more Dprs that bind DIP-β than L1 neurons during synapse formation. Additionally, it will be important to determine if Dpr and DIP proteins cluster together at developing L4-L2 synapses and interact with synaptic proteins. Given that Dprs and DIPs lack obvious intracellular signaling motifs and that many are predicted to be linked to the plasma membrane through a lipid anchor (Cheng et al., 2018), if they interact with synaptic machinery, then this would be likely to occur through co-receptors.

## DIP Mis-expression Changes the Synaptic Connections of L Cells in a Predictable Manner

Our mis-expression experiments support a role for DIPs-β and γ in promoting synapse formation with Dpr-expressing neurons. Interestingly, since L cells and R cells already contact each other extensively within cartridges, DIP mis-expression is unlikely to promote synapse formation by forcing contact between these neurons. Rather, DIP mis-expression may make L cells competent to synapse onto R cells and each other. We hypothesize that mis-expressing DIP-γ in R cells or L cells and mis-expressing DIP-β in L cells promotes *trans* interactions with cognate Dprs expressed in L cells that go on to recruit synaptic machinery resulting in synapse formation. However, it is possible that DIP proteins promote synapse formation independent of Dprs. Experiments eliminating the ability of DIPs-γ or β to bind Dprs or disrupting the function of Dprs that bind DIP-γ or β in L cells

**Table 1. Expression of Dprs that Bind DIP-β in L1 and L2 Neurons**

| Developmental Stage | Neuron Type | Dprs Expressed | | | | | |
|---|---|---|---|---|---|---|---|
| 40 h APF | L1 | Dpr10 (54.9) | Dpr15 (22) | Dpr21 (1.83) | | | |
| | L2 | Dpr6 (19.4) | Dpr8 (1.52) | Dpr9 (4.07) | Dpr10 (54.9) | Dpr11 (94) | Dpr21 (1.83) |
| 72 h APF | L1 | Dpr10 (54.9) | | | | | |
| | L2 | Dpr6 (19.4) | Dpr11 (94) | | | | |

The expression of Dprs that bind DIP-β in L1 and L2 neurons at 40 and 72 h APF as reported by Tan et al. (2015). The binding affinity of DIP-β for specific Dprs is shown in parentheses, represented as dissociation constants (μM) determined by Cosmanescu et al. (2018). The expression of Dprs 6, 10, 11, and 15 were assessed at the protein level. The expression of all other Dprs was examined at the mRNA level through RNA-seq.

are needed to determine whether specific Dpr-DIP interactions contribute to ectopic synapse formation in DIP mis-expression experiments. It is unclear why the mis-expression phenotypes are nonuniform (not all cartridges contain ectopic synapses). It is possible that synapse refinement contributes to the nonuniform pattern of ectopic synapse formation. For example, early in development, many cartridges may contain ectopic synapses that then become pruned away over time.

### Dpr-DIP Interactions May Regulate Synaptic Specificity by Establishing a Preference for Synaptic Partners

Synapse formation is robust (see also Hassan and Hiesinger, 2015). In both vertebrates and invertebrates, it has been shown that disrupting proteins known to regulate synapse organization (Chen et al., 2017; Mosca et al., 2012; Mosca and Luo, 2014; Robbins et al., 2010; Südhof, 2017; Varoqueaux et al., 2006) or specificity (Krishnaswamy et al., 2015; Shen and Bargmann, 2003; Shen et al., 2004) does not prevent neurons from forming synapses. In addition, in the absence of appropriate partners, neurons have the capacity to synapse with alternative partners (Bekkers and Stevens, 1991; Cash et al., 1992; Duan et al., 2014; Peng et al., 2018; Shen and Bargmann, 2003). The findings we report here are consistent with these observations. Collectively, our data support the idea that DIP proteins play an instructive role in establishing synaptic specificity but show that they are not necessary for synapse formation. Our working hypothesis is that interactions between DIP-β in L4 neurons and cognate Dprs in L2 neurons establish a preference for L4 to synapse onto L2 over other cell partnerships in the cartridge (Figure 5A). In the absence of this preference, L4 has the capacity to synapse with other cell types (e.g., L1). Similarly, mis-expression of DIP-γ in R cells or L cells and DIP-β in L cells establishes a preference for L cells to synapse with R cells or each other. Thus, we propose that when Dpr-DIP interactions are disrupted synapses still form but reflect a loss of preference for the correct partners and that inducing ectopic Dpr-DIP interactions introduces incorrect preferences that promote synapses to form between incorrect partners (Figure 5B). Similar models of synaptic specificity have been proposed in *C. elegans* and mice. In *C. elegans*, interactions between the IgSF proteins SYG-1, expressed in the HSNL neuron, and SYG-2, expressed in vulval epithelial cells (guidepost cells), restrict the subcellular location of synapse formation in HSNL, biasing HSNL to synapse with specific partners (Shen and Bargmann, 2003; Shen et al., 2004). An important difference between the SYG proteins and Dprs and DIPs is that Dpr-DIP interactions occur between synaptic partners rather than with guidepost cells. In the mouse retina, the IgSF protein Sdk2 regulates selective synapse formation between an interneuron and a retinal ganglion neuron after they have innervated the correct sublaminae (Krishnaswamy et al., 2015). It was proposed that Sdk2 and other similar molecules may bias synapses to form between specific cell types within sublaminae. Thus, our study, together with previous studies, suggests an evolutionarily shared strategy for establishing synaptic specificity.

## STAR★METHODS

Detailed methods are provided in the online version of this paper and include the following:

- KEY RESOURCES TABLE
- TABLE OF GENOTYPES - FULL GENOTYPES OF FLIES IN EACH EXPERIMENT
- LEAD CONTACT AND MATERIALS AVAILABILITY
- EXPERIMENTAL MODEL AND SUBJECT DETAILS
  - Experimental model used in this study- *Drosophila melanogaster*
- METHOD DETAILS
  - Production of DIP antibodies
  - Immunohistochemistry
  - Electron microscopy
  - Optomotor and phototaxis assays
  - Electroretinogram recordings
  - Machine learning algorithm for tracing cartridges and puncta
- QUANTIFICATION AND STATISTICAL ANALYSIS
  - Quantification of L2 and L4 cell numbers
  - Quantification of Brp puncta in the distal regions of lamina cartridges
  - Quantification of DIP-β fluorescence signal
  - Statistical Analysis of Brp puncta
  - Statistical analysis by figure
- DATA AND CODE AVAILABILITY

### SUPPLEMENTAL INFORMATION

Supplemental Information can be found online at https://doi.org/10.1016/j.neuron.2019.06.006.

### ACKNOWLEDGMENTS

We would like to thank Drs. Zipursky, Ginty, Kaeser, and Chen for many helpful discussions and comments on the manuscript. This research was supported

by NIH-NINDS (National Institute of Neurological Disorders and Stroke) grants K01 K01NS094545 (M.Y.P.), R01 1R01NS110713 (M.Y.P.), R01 NS103905 (M.Y.P.), and the McKnight Foundation (scholar award to M.Y.P.), and the Whitehall Foundation (research grant to M.Y.P.). C.X. was supported by an Alice and Joseph Brooks postdoctoral fellowship and an Edward R. and Anne G. Lefler Center postdoctoral fellowship.

## AUTHOR CONTRIBUTIONS

Conceptualization, M.Y.P. and C.X.; Methodology, M.Y.P., C.X., and R.M.; Validation, C.X., E.T., E.R., B.S., and R.M.; Software, C.Y., Formal Analysis, M.Y.P., C.X., E.T., R.M., Z.W., D.T., J.B., T.G., R.L., J.D., and I.A.M.; Investigation, C.X., E.T., R.M., Z.W., E.R., and D.T.; Resources, M.Y.P., I.A.M., B.d.B., J.P., L.T., and M.C.; Writing – Original Draft, M.Y.P.; Writing – Review & Editing, M.Y.P., C.X., E.T., I.A.M., B.d.B., Z.W., and R.M.; Visualization, M.Y.P., C.X., E.T., and R.M.; Supervision, M.Y.P. and C.X.; Project Administration, M.Y.P.; Funding Acquisition, M.Y.P.

## DECLARATION OF INTERESTS

The authors declare no competing interests.

Received: August 24, 2018
Revised: April 19, 2019
Accepted: June 11, 2019
Published: July 9, 2019; corrected online: April 9, 2020

## REFERENCES

Akin, O., and Zipursky, S.L. (2016). Frazzled promotes growth cone attachment at the source of a Netrin gradient in the *Drosophila* visual system. eLife *5*, e20762.

Ashley, J., Sorrentino, V., Nagarkar-Jaiswal, S., Tan, L., Xu, S., Xiao, Q., Zinn, K., and Carrillo, R.A. (2018). Transsynaptic interactions between IgSF proteins DIP-α and Dpr10 are required for motor neuron targeting specificity in *Drosophila*. bioRxiv. https://doi.org/10.1101/424416.

Ashley, J., Sorrentino, V., Lobb-Rabe, M., Nagarkar-Jaiswal, S., Tan, L., Xu, S., Xiao, Q., Zinn, K., and Carrillo, R.A. (2019). Transsynaptic interactions between IgSF proteins DIP-α and Dpr10 are required for motor neuron targeting specificity. eLife *8*, e42690.

Baier, H. (2013). Synaptic laminae in the visual system: molecular mechanisms forming layers of perception. Annu. Rev. Cell Dev. Biol. *29*, 385–416.

Barish, S., Nuss, S., Strunilin, I., Bao, S., Mukherjee, S., Jones, C.D., and Volkan, P.C. (2018). Combinations of DIPs and Dprs control organization of olfactory receptor neuron terminals in *Drosophila*. PLoS Genet. *14*, e1007560.

Bekkers, J.M., and Stevens, C.F. (1991). Excitatory and inhibitory autaptic currents in isolated hippocampal neurons maintained in cell culture. Proc. Natl. Acad. Sci. USA *88*, 7834–7838.

Braitenberg, V. (1967). Patterns of projection in the visual system of the fly. I. Retina-lamina projections. Exp. Brain Res. *3*, 271–298.

Cang, J., and Feldheim, D.A. (2013). Developmental mechanisms of topographic map formation and alignment. Annu. Rev. Neurosci. *36*, 51–77.

Carrillo, R.A., Özkan, E., Menon, K.P., Nagarkar-Jaiswal, S., Lee, P.T., Jeon, M., Birnbaum, M.E., Bellen, H.J., Garcia, K.C., and Zinn, K. (2015). Control of synaptic connectivity by a network of *Drosophila* IgSF cell surface proteins. Cell *163*, 1770–1782.

Cash, S., Chiba, A., and Keshishian, H. (1992). Alternate neuromuscular target selection following the loss of single muscle fibers in *Drosophila*. J. Neurosci. *12*, 2051–2064.

Chen, P.L., and Clandinin, T.R. (2008). The cadherin Flamingo mediates level-dependent interactions that guide photoreceptor target choice in *Drosophila*. Neuron *58*, 26–33.

Chen, Y., Akin, O., Nern, A., Tsui, C.Y., Pecot, M.Y., and Zipursky, S.L. (2014). Cell-type-specific labeling of synapses in vivo through synaptic tagging with recombination. Neuron *81*, 280–293.

Chen, L.Y., Jiang, M., Zhang, B., Gokce, O., and Sudhof, T.C. (2017). Conditional deletion of all neurexins defines diversity of essential synaptic organizer functions for neurexins. Neuron *94*, 611–62. e614.

Cheng, S., Park, Y., Kurleto, J.D., Jeon, M., Zinn, K., Thornton, J.W., and Ozkan, E. (2018). A new family of neural wiring receptors across bilaterians defined by phylogenetic, biochemical and structural evidence. bioRxiv. https://doi.org/10.1101/462036.

Cheng, S., Ashley, J., Kurleto, J.D., Lobb-Rabe, M., Park, Y.J., Carrillo, R.A., and Özkan, E. (2019). Molecular basis of synaptic specificity by immunoglobulin superfamily receptors in *Drosophila*. eLife *8*, e41028.

Choe, K.M., Prakash, S., Bright, A., and Clandinin, T.R. (2006). Liprin-alpha is required for photoreceptor target selection in *Drosophila*. Proc. Natl. Acad. Sci. USA *103*, 11601–11606.

Clandinin, T.R., and Zipursky, S.L. (2000). Afferent growth cone interactions control synaptic specificity in the *Drosophila* visual system. Neuron *28*, 427–436.

Clandinin, T.R., Lee, C.H., Herman, T., Lee, R.C., Yang, A.Y., Ovasapyan, S., and Zipursky, S.L. (2001). *Drosophila* LAR regulates R1-R6 and R7 target specificity in the visual system. Neuron *32*, 237–248.

Coombe, P.E. (1986). The large monopolar cells L1 and L2 are responsible for ERG transients in *Drosophila*. J. Comp. Physiol. A Neuroethol. Sens. Neural Behav. Physiol. *159*, 655–665.

Cosmanescu, F., Katsamba, P.S., Sergeeva, A.P., Ahlsen, G., Patel, S.D., Brewer, J.J., Tan, L., Xu, S., Xiao, Q., Nagarkar-Jaiswal, S., et al. (2018). Neuron-subtype-specific expression, interaction affinities, and specificity determinants of DIP/Dpr cell recognition proteins. Neuron *100*, 1385–1400.e1386.

Duan, X., Krishnaswamy, A., De la Huerta, I., and Sanes, J.R. (2014). Type II cadherins guide assembly of a direction-selective retinal circuit. Cell *158*, 793–807.

Feldheim, D.A., and O'Leary, D.D. (2010). Visual map development: bidirectional signaling, bifunctional guidance molecules, and competition. Cold Spring Harb. Perspect. Biol. *2*, a001768.

Flanagan, J.G. (2006). Neural map specification by gradients. Curr. Opin. Neurobiol. *16*, 59–66.

Golic, K.G., and Lindquist, S. (1989). The FLP recombinase of yeast catalyzes site-specific recombination in the *Drosophila* genome. Cell *59*, 499–509.

Hassan, B.A., and Hiesinger, P.R. (2015). Beyond molecular codes: simple rules to wire complex brains. Cell *163*, 285–291.

Heisenberg, M. (1971). Separation of receptor and lamina potentials in the electroretinogram of normal and mutant *Drosophila*. J. Exp. Biol. *55*, 85–100.

Hong, W., Mosca, T.J., and Luo, L. (2012). Teneurins instruct synaptic partner matching in an olfactory map. Nature *484*, 201–207.

Huber, A.B., Kolodkin, A.L., Ginty, D.D., and Cloutier, J.F. (2003). Signaling at the growth cone: ligand-receptor complexes and the control of axon growth and guidance. Annu. Rev. Neurosci. *26*, 509–563.

Huberman, A.D., Clandinin, T.R., and Baier, H. (2010). Molecular and cellular mechanisms of lamina-specific axon targeting. Cold Spring Harb. Perspect. Biol. *2*, a001743.

Kirschfeld, K. (1967). Die Projektion der optischen Umwelt auf das Raster der Rhabdomere im Komplexauge von MUSCA. Exp. Brain Res. *3*, 248–270.

Kolodkin, A.L., and Tessier-Lavigne, M. (2011). Mechanisms and molecules of neuronal wiring: a primer. Cold Spring Harb. Perspect. Biol. *3*, a001727.

Krishnaswamy, A., Yamagata, M., Duan, X., Hong, Y.K., and Sanes, J.R. (2015). Sidekick 2 directs formation of a retinal circuit that detects differential motion. Nature *524*, 466–470.

Lai, S.L., and Lee, T. (2006). Genetic mosaic with dual binary transcriptional systems in *Drosophila*. Nat. Neurosci. *9*, 703–709.

Langen, M., Agi, E., Altschuler, D.J., Wu, L.F., Altschuler, S.J., and Hiesinger, P.R. (2015). The developmental rules of neural superposition in *Drosophila*. Cell *162*, 120–133.

Langley, J.N. (1895). Note on regeneration of prae-ganglionic fibres of the sympathetic. J. Physiol. *18*, 280–284.

Lee, C.H., Herman, T., Clandinin, T.R., Lee, R., and Zipursky, S.L. (2001). N-cadherin regulates target specificity in the *Drosophila* visual system. Neuron *30*, 437–450.

Lee, R.C., Clandinin, T.R., Lee, C.H., Chen, P.L., Meinertzhagen, I.A., and Zipursky, S.L. (2003). The protocadherin Flamingo is required for axon target selection in the *Drosophila* visual system. Nat. Neurosci. *6*, 557–563.

Lüthy, K., Ahrens, B., Rawal, S., Lu, Z., Tarnogorska, D., Meinertzhagen, I.A., and Fischbach, K.F. (2014). The irre cell recognition module (IRM) protein Kirre is required to form the reciprocal synaptic network of L4 neurons in the *Drosophila* lamina. J. Neurogenet. *28*, 291–301.

Meinertzhagen, I.A. (1996). Ultrastructure and quantification of synapses in the insect nervous system. J. Neurosci. Methods *69*, 59–73.

Meinertzhagen, I.A., and O'Neil, S.D. (1991). Synaptic organization of columnar elements in the lamina of the wild type in *Drosophila* melanogaster. J. Comp. Neurol. *305*, 232–263.

Mosca, T.J., and Luo, L. (2014). Synaptic organization of the *Drosophila* antennal lobe and its regulation by the Teneurins. eLife *3*, e03726.

Mosca, T.J., Hong, W., Dani, V.S., Favaloro, V., and Luo, L. (2012). Trans-synaptic Teneurin signalling in neuromuscular synapse organization and target choice. Nature *484*, 237–241.

Nakamura, M., Baldwin, D., Hannaford, S., Palka, J., and Montell, C. (2002). Defective proboscis extension response (DPR), a member of the Ig superfamily required for the gustatory response to salt. J. Neurosci. *22*, 3463–3472.

Newsome, T.P., Asling, B., and Dickson, B.J. (2000). Analysis of *Drosophila* photoreceptor axon guidance in eye-specific mosaics. Development *127*, 851–860.

Özkan, E., Carrillo, R.A., Eastman, C.L., Weiszmann, R., Waghray, D., Johnson, K.G., Zinn, K., Celniker, S.E., and Garcia, K.C. (2013). An extracellular interactome of immunoglobulin and LRR proteins reveals receptor-ligand networks. Cell *154*, 228–239.

Pecot, M.Y., Tadros, W., Nern, A., Bader, M., Chen, Y., and Zipursky, S.L. (2013). Multiple interactions control synaptic layer specificity in the *Drosophila* visual system. Neuron *77*, 299–310.

Peng, J., Santiago, I.J., Ahn, C., Gur, B., Tsui, C.K., Su, Z., Xu, C., Karakhanyan, A., Silies, M., and Pecot, M.Y. (2018). *Drosophila* Fezf coordinates laminar-specific connectivity through cell-intrinsic and cell-extrinsic mechanisms. eLife *7*, e33962.

Prakash, S., Caldwell, J.C., Eberl, D.F., and Clandinin, T.R. (2005). *Drosophila* N-cadherin mediates an attractive interaction between photoreceptor axons and their targets. Nat. Neurosci. *8*, 443–450.

Rivera-Alba, M., Vitaladevuni, S.N., Mishchenko, Y., Lu, Z., Takemura, S.Y., Scheffer, L., Meinertzhagen, I.A., Chklovskii, D.B., and de Polavieja, G.G. (2011). Wiring economy and volume exclusion determine neuronal placement in the *Drosophila* brain. Curr. Biol. *21*, 2000–2005.

Robbins, E.M., Krupp, A.J., Perez de Arce, K., Ghosh, A.K., Fogel, A.I., Boucard, A., Südhof, T.C., Stein, V., and Biederer, T. (2010). SynCAM 1 adhesion dynamically regulates synapse number and impacts plasticity and learning. Neuron *68*, 894–906.

Sanes, J.R., and Yamagata, M. (1999). Formation of lamina-specific synaptic connections. Curr. Opin. Neurobiol. *9*, 79–87.

Schindelin, J., Arganda-Carreras, I., Frise, E., Kaynig, V., Longair, M., Pietzsch, T., Preibisch, S., Rueden, C., Saalfeld, S., Schmid, B., et al. (2012). Fiji: an open-source platform for biological-image analysis. Nat. Methods *9*, 676–682.

Schwabe, T., Neuert, H., and Clandinin, T.R. (2013). A network of cadherin-mediated interactions polarizes growth cones to determine targeting specificity. Cell *154*, 351–364.

Schwabe, T., Borycz, J.A., Meinertzhagen, I.A., and Clandinin, T.R. (2014). Differential adhesion determines the organization of synaptic fascicles in the *Drosophila* visual system. Curr. Biol. *24*, 1304–1313.

Shen, K., and Bargmann, C.I. (2003). The immunoglobulin superfamily protein SYG-1 determines the location of specific synapses in C. elegans. Cell *112*, 619–630.

Shen, K., Fetter, R.D., and Bargmann, C.I. (2004). Synaptic specificity is generated by the synaptic guidepost protein SYG-2 and its receptor, SYG-1. Cell *116*, 869–881.

Sperry, R.W. (1963). Chemoaffinity in the orderly growth of nerve fiber patterns and connections. Proc. Natl. Acad. Sci. USA *50*, 703–710.

Südhof, T.C. (2017). Synaptic neurexin complexes: a molecular code for the logic of neural circuits. Cell *171*, 745–769.

Tan, L., Zhang, K.X., Pecot, M.Y., Nagarkar-Jaiswal, S., Lee, P.T., Takemura, S.Y., McEwen, J.M., Nern, A., Xu, S., Tadros, W., et al. (2015). Ig superfamily ligand and receptor pairs expressed in synaptic partners in *Drosophila*. Cell *163*, 1756–1769.

Tessier-Lavigne, M., and Goodman, C.S. (1996). The molecular biology of axon guidance. Science *274*, 1123–1133.

Tuthill, J.C., Nern, A., Holtz, S.L., Rubin, G.M., and Reiser, M.B. (2013). Contributions of the 12 neuron classes in the fly lamina to motion vision. Neuron *79*, 128–140.

Varoqueaux, F., Aramuni, G., Rawson, R.L., Mohrmann, R., Missler, M., Gottmann, K., Zhang, W., Südhof, T.C., and Brose, N. (2006). Neuroligins determine synapse maturation and function. Neuron *51*, 741–754.

Venkatasubramanian, L., Guo, Z., Xu, S., Tan, L., Xiao, Q., Nagarkar-Jaiswal, S., and Mann, R.S. (2019). Stereotyped terminal axon branching of leg motor neurons mediated by IgSF proteins DIP-α and Dpr10. eLife *8*, e42692.

Wagh, D.A., Rasse, T.M., Asan, E., Hofbauer, A., Schwenkert, I., Dürrbeck, H., Buchner, S., Dabauvalle, M.C., Schmidt, M., Qin, G., et al. (2006). Bruchpilot, a protein with homology to ELKS/CAST, is required for structural integrity and function of synaptic active zones in *Drosophila*. Neuron *49*, 833–844.

Werkhoven, Z., Rohrsen, C., Qin, C., Brems, B., and de Bivort, B. (2019). MARGO (massively automated real-time GUI for object-tracking), a platform for high-throughput ethology. bioRxiv. https://doi.org/10.1101/593046.

Xu, S., Xiao, Q., Cosmanescu, F., Sergeeva, A.P., Yoo, J., Lin, Y., Katsamba, P.S., Ahlsen, G., Kaufman, J., Linaval, N.T., et al. (2018). Interactions between the Ig-superfamily proteins DIP-alpha and Dpr6/10 regulate assembly of neural circuits. Neuron *100*, 1369–1384.e1366.

Zhang, K.X., Tan, L., Pellegrini, M., Zipursky, S.L., and McEwen, J.M. (2016). Rapid changes in the translatome during the conversion of growth cones to synaptic terminals. Cell Rep. *14*, 1258–1271.

Zinn, K., and Özkan, E. (2017). Neural immunoglobulin superfamily interaction networks. Curr. Opin. Neurobiol. *45*, 99–105.

## STAR★METHODS

### KEY RESOURCES TABLE

| REAGENT or RESOURCE | SOURCE | IDENTIFIER |
|---|---|---|
| Experimental Models: Organisms/Strains | | |
| Strain (*Drosophila melanogaster*) 48A08AD (II), 66A01DBD (III) [L1 split-GAL4] | Janelia Research Campus (Tuthill et al., 2013) | N/A |
| Strain (*Drosophila melanogaster*) 53G02AD (II), 29G11DBD (III) [L2 split-GAL4] | Janelia Research Campus (Tuthill et al., 2013) | N/A |
| Strain (*Drosophila melanogaster*) 64B03AD (II), 14B07DBD (III) [L3 split-GAL4] | Janelia Research Campus (Tuthill et al., 2013) | N/A |
| Strain (*Drosophila melanogaster*) 31C06AD (III), 34G07DBD (III), [L4 split-GAL4] | Janelia Research Campus (Tuthill et al., 2013) | N/A |
| Strain (*Drosophila melanogaster*) 64D07AD (II), 37E10DBD (III) [L5 split-GAL4] | Janelia Research Campus (Tuthill et al., 2013) | N/A |
| Strain (*Drosophila melanogaster*) 79C23S-GS-FRT-stop-FRT-smFPV5-2A-LexAVP16 | J. Peng (Peng et al., 2018) | N/A |
| Strain (*Drosophila melanogaster*) LexAop-myr::tdTomato (III) | Akin and Zipursky, 2016 | N/A |
| Strain (*Drosophila melanogaster*) UAS-Flp (II) | Bloomington Drosophila Stock Center | RRID:BDSC_4540 |
| Strain (*Drosophila melanogaster*) 27G05-FLPG5.PEST (attp5) | Janelia research campus (Peng et al., 2018) | N/A |
| Strain (*Drosophila melanogaster*) GMR-GAL4 (III) | Bloomington Drosophila Stock Center | RRID:BDSC_8121 |
| Strain (*Drosophila melanogaster*) 27G05-GAL4 (attp2) | Bloomington Drosophila Stock Center | RRID:BDSC_48703 |
| Strain (*Drosophila melanogaster*) UAS-β-RNAi (attp40) | Bloomington Drosophila Stock Center | RRID:BDSC_38310 |
| Strain (*Drosophila melanogaster*) 9B08GAL4 | (Pecot et al., 2013) | N/A |
| Strain (*Drosophila melanogaster*) DIP-$\beta^{1-95}$ | This study | N/A |
| Strain (*Drosophila melanogaster*) DIP-$\gamma^{1-67}$ | This study | N/A |
| Strain (*Drosophila melanogaster*) UAS-DIP-γ | This study | N/A |
| Strain (*Drosophila melanogaster*) UAS-DIP-ε | This study | N/A |
| Strain (*Drosophila melanogaster*) UAS-DIP-β | This study | N/A |
| Antibodies | | |
| Antibody Anti-V5 (mouse) 1:200 | Bio-Rad/AbD Serotec | Cat# MCA2892GA; RRID:AB_1658039 |
| Antibody Anti-DsRed (rabbit) 1:200 | Clontech Laboratories, Inc. | Cat# 632496; RRID:AB_10013483 |
| Antibody anti-chaoptin (mouse) 1:20 | Developmental Studies Hybridoma Bank | Cat# 24B10, RRID:AB_528161 |
| Antibody Anti-DIP-Beta (guinea pig) 1:300 | This study | N/A |
| Antibody Anti-DIP-Epsilon (rabbit) 1:500 | This study | N/A |
| Antibody Anti-DIP-Gamma (guinea pig) 1:400 | This study | N/A |
| Antibody Goat anti-Mouse IgG (H&L) Highly Cross-Adsorbed Secondary Antibody, Alexa Fluor 488 1:500 | Thermo Fisher Scientific | Cat# A11029, RRID: AB_2534088 |
| Antibody Goat anti-Rabbitt IgG, Alexa Fluor 647 1:500 | Thermo Fisher Scientific | Cat# A21245, RRID: AB_2535813 |
| Antibody 647 Goat anti-Guinea Pig IgG (H&L) Highly Cross-Adsorbed Secondary Antibody, Alexa Fluor 647 1:500 | Thermo Fisher Scientific | Cat# A21450, RRID: AB_2535867 |

(*Continued on next page*)

*Continued*

| REAGENT or RESOURCE | SOURCE | IDENTIFIER |
|---|---|---|
| Software and Algorithms | | |
| Cartridge tracing algorithm | This paper | https://hms-idac.github.io/VoxelClassifier/ |
| MATLAB | Mathworks | https://www.mathworks.com/products/matlab.html |
| Prism | Graphpad | https://www.graphpad.com/scientific-software/prism/ |
| Fiji | Schindelin et al., 2012 | https://fiji.sc/ |
| R https://www.r-project.org/ | R core team (2013) | https://www.r-project.org/ |

## TABLE OF GENOTYPES - FULL GENOTYPES OF FLIES IN EACH EXPERIMENT

| RELEVANT FIGURES | ABBREVIATED NAMES | GENOTYPES |
|---|---|---|
| **Figure 1** | | |
| D,F | WT | w; Bl/Cyo; TM2/TM6B |
| E | β KO | DIP-$\beta^{1-95}$; +/+; +/+ |
| G | γ KO | w; Bl/Cyo; DIP-$\gamma^{1-67}$ |
| H, I, J, K, L | WT | w ;79C23S-GS-FRT-stop-FRT-GFPv5-2A-LexAVP16 (VK1); +/+ |
| H, I, J, K, L | DKO | DIP-$\beta^{1-95}$; 79C23S-GS-FRT-stop-FRT-GFPv5-2A-LexAVP16 (VK1); DIP-$\gamma^{1-67}$ |
| M, M', O, P, Q, R | WT | w; 79C23S-GS-FRT-stop-FRT-GFPv5-2A-LexAVP16 (VK1)/27G05FLP; LexAop-myr::tdTomato/TM2(TM6B) |
| N, N', O, P, Q, R | DKO | DIP-$\beta^{1-95}$; 79C23S-GS-FRT-stop-FRT-GFPv5-2A-LexAVP16 (VK1)/27G05FLP; LexAop-myr::tdTomato, DIP-$\gamma^{1-67}$/DIP-$\gamma^{1-67}$ |
| O, P, Q | DIP-γ (+/–) | w; 79C23S-GS-FRT-stop-FRT-GFPv5-2A-LexAVP16 (VK1)/27G05FLP; DIP-$\gamma^{1-67}$, LexAop-myr::tdTomato/TM2(TM6B) |
| O, P, Q | DIP-γ (–/–) | w; 79C23S-GS-FRT-stop-FRT-GFPv5-2A-LexAVP16 (VK1)/27G05FLP; DIP-$\gamma^{1-67}$, LexAop-myr::tdTomato/ DIP-$\gamma^{1-67}$ |
| O, P, Q | DIP-β (+/–) | DIP-$\beta^{1-95}$/w; 79C23S-GS-FRT-stop-FRT-GFPv5-2A-LexAVP16 (VK1)/27G05FLP; LexAop-myr::tdTomato/TM2(TM6B) |
| O, P, Q | DIP-β (–/–) | DIP-$\beta^{1-95}$; 79C23S-GS-FRT-stop-FRT-GFPv5-2A-LexAVP16 (VK1)/27G05FLP; LexAop-myr::tdTomato/TM2(TM6B) |
| **Figure 2** | | |
| A, A', B, B', D, E, F, G, H | WT | w; UAS-FLP/+ ; 31C06AD, 34G07DBD/79C23S-GS-FRT-stop-FRT-GFPv5-2A-LexAVP16 (VK1), LexAop-myr::tdTomato |
| C, C', D, E, F, G, H | DKO | DIP-$\beta^{1-95}$; UAS-FLP, 79C23S-GS-FRT-stop-FRT-GFPv5-2A-LexAVP16 (VK1)/+ ; 31C06AD, 34G07DBD, DIP-$\gamma^{1-67}$/ DIP-$\gamma^{1-67}$, LexAop-myr::tdTomato |
| I, J, K, M, N, O | WT | w; UAS-FLP/+ ; 31C06AD, 34G07DBD/ 79C23S-GS-FRT-stop-FRT-GFPv5-2A-LexAVP16 (VK1), LexAop-myr::tdTomato |
| I, J, K, L, M, N, O | DIP-β (–/–) | DIP-$\beta^{1-95}$; UAS-FLP/+ ; 31C06AD, 34G07DBD/ 79C23S-GS-FRT-stop-FRT-GFPv5-2A-LexAVP16 (VK1), LexAop-myr::tdTomato |
| **Figure 3** | | |
| A | WT | w; Bl/CyO; TM2/TM6B |
| B | β-KO | DIP-$\beta^{1-95}$; +/+; +/+ |
| C, C' | CTL | w; UAS-DIP-βRNAi/Bl(CyO); +/TM2(TM6B) |
| D, D' | β-cKD | w; UAS-DIP-βRNAi/Bl(CyO); 9B08GAL4/TM2(TM6B) |
| E, F, G | CTL | w; UAS-DIP-βRNAi/27G05FLP; 79C23S-GS-FRT-stop-FRT-GFPv5-2A-LexAVP16 (VK1),LexAopmyr::tdTomato/ TM6B |

(*Continued on next page*)

*Continued*

| RELEVANT FIGURES | ABBREVIATED NAMES | GENOTYPES |
|---|---|---|
| E, F, G | β-cKD | w; UAS-DIP-βRNAi/27G05FLP; 79C23S-GS-FRT-stop-FRT-GFPv5-2A-LexAVP16 (VK1),LexAopmyr::tdTomato/ 9B08GAL4 |
| H, H', I, I', J, J', J'' | WT | w; 27G05FLP/BI(CyO); 79C23S-GS-FRT-stop-FRT-GFPv5-2A-LexAVP16, LexAop-myr::tdTomato/TM2 |
| **Figure 4** | | |
| A, A', D | CTL | w; UAS-DIP-γ/27G05FLP; 79C23S-GS-FRT-stop-FRT-GFPv5-2A-LexAVP16, LexAop-myr::tdTomato/TM2(TM6B) |
| B, B', C, D | R cells-DIP-γ | w; UAS-DIP-γ/27G05FLP; 79C23S-GS-FRT-stop-FRT-GFPv5-2A-LexAVP16, LexAop-myr::tdTomato/GMR-GAL4 |
| E, E', H | CTL | w; BI(Cyo)/27G05FLP; 79C23S-GS-FRT-stop-FRT-GFPv5-2A-LexAVP16, LexAop-myr::tdTomato/27G05-GAL4 |
| F, F', G, H | L cells-DIP-γ | w; UAS-DIP-γ/27G05FLP; 79C23S-GS-FRT-stop-FRT-GFPv5-2A-LexAVP16, LexAop-myr::tdTomato/27G05-GAL4 |
| I, I', L | CTL | w; 79C23S-GS-FRT-stop-FRT-GFPv5-2A-LexAVP16, LexAop-myr::tdTomato/27G05FLP; UAS-DIP-β/TM2(TM6B) |
| J, J', K, L | L cells-DIP-β | w; 79C23S-GS-FRT-stop-FRT-GFPv5-2A-LexAVP16, LexAop-myr::tdTomato/27G05FLP; UAS-DIP-β/27G05GAL4 |
| M, N | L cells-DIP-γ, ε | w; UAS-DIP-γ, UAS-DIP-ε/27G05FLP; 79C23S-GS-FRT-stop-FRT-GFPv5-2A-LexAVP16, LexAop-myr::tdTomato/GMR-GAL4 |
| Figure S1 | | |
| B, C, D, E, F | WT | w ;79C23S-GS-FRT-stop-FRT-GFPv5-2A-LexAVP16 (VK1); +/+ |
| B, C, D, E, F | DKO | DIP-$\beta^{1-95}$; 79C23S-GS-FRT-stop-FRT-GFPv5-2A-LexAVP16 (VK1); DIP-$\gamma^{1-67}$ |
| G | WT | w; BI/CyO; TM2/TM6B |
| H | DIP-β (+/−) | DIP-$\beta^{1-95}$/w; +/BI(CyO); +/TM2(TM6B) |
| Figure S2 | | |
| A, A' | CTL | DIP-$\beta^{1-95}$/w; UAS-Flp, 79C23S-GS-FRT-stop-FRT-GFPv5-2A-LexAVP16 (VK1)/48A08AD; 66A01DBD/ DIP-$\gamma^{1-67}$, LexAop-myr::tdTomato |
| B, B' | DKO | DIP-$\beta^{1-95}$; UAS-Flp, 79C23S-GS-FRT-stop-FRT-GFPv5-2A-LexAVP16 (VK1)/48A08AD; 66A01DBD, DIP-$\gamma^{1-67}$/ DIP-$\gamma^{1-67}$, LexAop-myr::tdTomato |
| C, C' | CTL | DIP-$\beta^{1-95}$/w; UAS-Flp, 79C23S-GS-FRT-stop-FRT-GFPv5-2A-LexAVP16 (VK1)/64B03AD; 14B07DBD/ DIP-$\gamma^{1-67}$, LexAop-myr::tdTomato |
| D, D' | DKO | DIP-$\beta^{1-95}$; UAS-Flp, 79C23S-GS-FRT-stop-FRT-GFPv5-2A-LexAVP16 (VK1)/64B03AD; 14B07DBD, DIP-$\gamma^{1-67}$/ DIP-$\gamma^{1-67}$, LexAop-myr::tdTomato |
| E, E' | WT | w; UAS-Flp/64D07AD; 37E10DBD/79C23S-GS-FRT-stop-FRT-GFPv5-2A-LexAVP16 (VK1), LexAop-myr::tdTomato |
| F, F' | DKO | DIP-$\beta^{1-95}$; UAS-Flp/64D07AD; 37E10DBD, DIP-$\gamma^{1-67}$/ DIP-$\gamma^{1-67}$, 79C23S-GS-FRT-stop-FRT-GFPv5-2A-LexAVP16 (VK1), LexAop-myr::tdTomato |
| G, G', I, J, K | WT | w; UAS-Flp/53G02AD; 29G11DBD/79C23S-GS-FRT-stop-FRT-GFPv5-2A-LexAVP16 (VK1), LexAop-myr::tdTomato |
| H, H', I, J, K | DKO | DIP-$\beta^{1-95}$; UAS-Flp/53G02AD; 29G11DBD, DIP-$\gamma^{1-67}$/ DIP-$\gamma^{1-67}$, 79C23S-GS-FRT-stop-FRT-GFPv5-2A-LexAVP16 (VK1), LexAop-myr::tdTomato |
| L | WT | w; UAS-FLP/+ ; 31C06AD, 34G07DBD/79C23S-GS-FRT-stop-FRT-GFPv5-2A-LexAVP16 (VK1), LexAop-myr::tdTomato |
| M | DKO | DIP-$\beta^{1-95}$; UAS-FLP, 79C23S-GS-FRT-stop-FRT-GFPv5-2A-LexAVP16 (VK1)/+ ; 31C06AD, 34G07DBD, DIP-$\gamma^{1-67}$/ DIP-$\gamma^{1-67}$, LexAop-myr::tdTomato |

(*Continued on next page*)

| *Continued* | | |
|---|---|---|
| RELEVANT FIGURES | ABBREVIATED NAMES | GENOTYPES |
| Figure S3 | | |
| A, B | WT | w; BI/Cyo; TM2/TM6B |
| C, C', C'' | CTL | yv/w; UAS-βRNAi/BI(CyO); +/TM2(TM6B) |
| D, D', D'' | β-cKD | w; UAS-βRNAi/BI(CyO); 31C06AD, 34G07DBD/+ |
| E, E', F, F' | 79h APF, 100h APF (new adult) | w; BI(Cyo)/27G05FLP; 79C23S-GS-FRT-stop-FRT-GFPv5-2A-LexAVP16, LexAop-myr::tdTomato/TM2 |
| Figure S4 | | |
| A, A' | R cells-DIP-γ,ε | w; UAS-DIP-γ, UAS-DIP-ε/27G05FLP; 79C23S-GS-FRT-stop-FRT-GFPv5-2A-LexAVP16, LexAop-myr::tdTomato/GMR-GAL4 |
| B, B' | R cells-DIP-ε | w; UAS-DIP-ε/27G05FLP; 79C23S-GS-FRT-stop-FRT-GFPv5-2A-LexAVP16, LexAop-myr::tdTomato/GMR-GAL4 |
| C, D | 48h APF | w; UAS-DIP-γ, UAS-DIP-ε/27G05FLP; 79C23S-GS-FRT-stop-FRT-GFPv5-2A-LexAVP16, LexAop-myr::tdTomato/GMR-GAL4 |
| E | CTL | w; BI(CyO)/27G05FLP; 79C23S-GS-FRT-stop-FRT-GFPv5-2A-LexAVP16, LexAop-myr::tdTomato/GMR-GAL4 |
| F | R Cells-DIP-γ | w; UAS-DIP-γ/27G05FLP; 79C23S-GS-FRT-stop-FRT-GFPv5-2A-LexAVP16, LexAop-myr::tdTomato/GMR-GAL4 |
| G, G' | R Cells-DIP-β | w; 79C23S-GS-FRT-stop-FRT-GFPv5-2A-LexAVP16, LexAop-myr::tdTomato/27G05FLP; UAS-DIP-β/GMRGAL4 |
| Figure S5 | | |
| | | w; UAS-DIP-γ, UAS-DIP-ε/27G05FLP; 79C23S-GS-FRT-stop-FRT-GFPv5-2A-LexAVP16, LexAop-myrtd::Tomato/GMR-GAL4 |
| Table S1 | | |
| | | w; UAS-DIP-γ, UAS-DIP-ε/27G05FLP; 79C23S-GS-FRT-stop-FRT-GFPv5-2A-LexAVP16, LexAop-myrtd::Tomato/GMR-GAL4 |

## LEAD CONTACT AND MATERIALS AVAILABILITY

Further information and requests for resources and reagents should be directed to and will be fulfilled by the Lead Contact, Matt Pecot (matthew_pecot@hms.harvard.edu). Antibodies and fly lines generated in this study will be distributed upon request.

## EXPERIMENTAL MODEL AND SUBJECT DETAILS

### Experimental model used in this study- *Drosophila melanogaster*

Flies were raised on standard cornmeal-agar based medium and maintained at 25°C with 50%–60% humidity. Male and female flies were used at the following developmental stages: 24h APF (after puparium formation), 48h APF, 72h APF, young adult (1-2 days-old), adult (~2 weeks old).

## METHOD DETAILS

### Production of DIP antibodies

***DIP-γ antigen: (aa22-393) full length except the predicted signal peptide and the TM domain (guinea pig)***

GSTQNQHHESSSQLDPDPEFIGFINNVTYPAGREAILACSVRNLGKNKVGWLRASDQTVLALQGRVVTHNARISVMHQDMHTWKLKIS
KLRESDRGCYMCQINTSPMKKQVGCIDVQVPPDIINEESSADLAVQEGEDATLTCKATGNPQPRVTWRREDGEMILIRKPGSRELMKVE
SYNGSSLRLLRLERRQMGAYLCIASNDVPPAVSKRVSLSVQFAPMVRAPSQLLGTPLGSDVQLECQVEASPSPVSYWLKGARTSNGFA
SVSTASLESGSPGPEMLLDGPKYGITERRDGYRGVMLLVVRSFSPSDVGTYHCVSTNSLGRAEGTLRLYEIKLHPGASASNDDHLNYIG
GLEEAARNAGRSNRTTWQ

***DIP-β antigen: (88-470aa) full length except a few AAs of the predicted signal peptide and the TM domain (guinea pig)***

NKISSVGAFEPDFVIPLENVTIAQGRDATFTCVVNNLGGHRVSGDGSSAPAKVAWIKADAKAILAIHEHVITNNDRLSVQHNDYNTWTLNI
RGVKMEDAGKYMCQVNTDPMKMQTATLEVVIPPDIINEETSGDMMVPEGGSAKLVCRARGHPKPKITWRREDGREIIARNGSHQKTKA
QSVEGEMLTLSKITRSEMGAYMCIASNGVPPTVSKRMKLQVHFHPLVQVPNQLVGAPVLTDVTLICNVEASPKAINYWQRENGEMIIAG
DRYALTEKENNMYAIEMILHIKRLQSSDFGGYKCISKNSIGDTEGTIRLYEMERPGKKILRDDDLNEVSKNEVVQKDTRSEDGSRNLNGR
LYKDRAPDQHPASGSDQLLGRGTMR

***DIP-ε antigen: (249-444aa)***

VDFSPMVWIPHQLVGIPIGFNITLECFIEANPTSLNYWTRENDQMITESSKYKTETIPGHPSYKATMRLTITNVQSSDYGNYKCVAKNPRG
DMDGNIKLYMSSPPTTQPPPTTTTLRRTTTTAAEIALDGYINTPLNGNGIGIVGEGPTNSVIASGKSSIKYLSNLNEIDKSKQKLTGSSPKG
FDWSKGKSSGSHG

Antigens and antibodies were produced at Genescript.

## Immunohistochemistry

Fly brains were dissected in Schneider's medium and fixed in 4% paraformaldehyde in phosphate buffered lysine for 25 min. After fixation, brains were quickly washed with phosphate buffer saline (PBS) with 0.5% Triton X-100 (PBT) and incubated in PBT for at least 2 hr at room temperature. Next, brains were incubated in blocking buffer (10% NGS, 0.5% Triton X-100 in PBS) overnight at 4°C. Brains were then incubated in primary antibody (diluted in blocking buffer) at 4°C for at least two nights. Following primary antibody incubation, brains were washed with PBT three times, 1 hr per wash. Next, brains were incubated in secondary antibody (diluted in blocking buffer) at 4°C for at least two nights. Following secondary antibody incubation, brains were washed with PBT two times, followed by one wash in PBS, 1 hr per wash. Finally, brains were mounted in SlowFade Gold antifade reagent (Thermo Fisher Scientific, Waltham, MA).

Confocal imaging was accomplished using either a Leica SP8 laser scanning confocal microscope or a Zeiss LSM800 Laser Scanning Microscope.

## Electron microscopy

The heads of 6-day old flies were dissected, immersed in a cacodylate-buffered paraformaldehyde and glutaraldehyde primary fixative, and processed for EM, as previously reported (Meinertzhagen and O'Neil, 1991; Meinertzhagen, 1996). Sections from Epon embedded specimens were cut serially at 60 nm, stained with 4% aqueous uranyl acetate and viewed with a FEI Tecnai 12 electron microscope operated at 80kV, and images collected with a Gatan 832 digital camera. A series of 500 consecutive sections in total was cut, 320 of which were imaged, aligned in ImageJ, and profiles identified and synapses marked manually.

## Optomotor and phototaxis assays

Behavioral assays were performed using the MARGO platform as described previously (Werkhoven et al., 2019). Briefly, co-housed DKO and CTL flies were transferred to individual optomotor (Figure 1H) or phototactic y-maze (Figure 1I) arenas. In the optomotor assay, fly location was tracked and a rotating pinwheel stimuli was centered on the fly (angular speed of 320 deg/s, spatial frequency of 0.02 cycles/deg). Optomotor index was measured as the fraction of angular movement of the fly occurring in the direction of the stimuli, normalize between 1 (all movement in the direction of the stimuli) and −1 (all movement occurring in the direction opposing the stimuli). In the phototactic Y-maze assay, flies were placed in a y-maze with an LED at the end of each arm as their location was tracked. Intensity ranged from 940.3 nW to 11.35 mW as measured by an optical power meter (400nm, ThorLabs). As the fly approached the center of the arena, the LED appeared at the end of one of the non-occupied arms of the Y-maze. Phototactic choice probability was calculated by measuring the percentage of trials in which the fly chose the lit arm of the Y-maze.

## Electroretinogram recordings

Electroretinogram recordings were performed on female flies using pairs of pulled glass electrodes (Sutter) filled with physiological *Drosophila* saline (103mM NaCl, 3 mM KCl, 5mM TES, 9 mM trehalos, 10mM glucose, 26mM $NaHCO_3$, 1 mM $NaH_2PO_4$, 4mM $MgCl_2$, 1.5 mM $CaCl_2$). One electrode was placed on the surface of the cornea while the other was impaled in the thorax of the fly. Stimuli were generated by a white LED (ThorLabs) and delivered through the optics of the microscope. Stimuli were shaped by inserting neutral density filters to adjust the intensity of the light: intensity ranged from 33.5mW at ND0 to 475μW as measured by an optical power meter (400nm, ThorLabs). Data were acquired using an A-M Model 3000 extracellular amplifier, digitized at 20,000 Hz using an Instrutech-ITC18 digitizer and acquired using Igor Pro 7. ERG waveforms were low pass filtered at 1000Hz and down-sampled to 500Hz for analysis—all ERG analysis was performed with custom MATLAB scripts. Differences between DKO and control flies were tested using a likelihood-ratio test of two linear mixed effects models (using the compare and fitlme() functions in MATLAB) on three measures of the ERG waveform, the steady state voltage (indicative of photoreceptor response, measured as the mean voltage in the final 0.25 s of the light step), and the on and off transient response (indicative of L1 and L2 response; the on response was measured as the maximum positive deflection within 0.1 s relative to the voltage before the stimulus, the off response was measured as the minimum voltage in the 0.1 s following light offset relative to the steady state voltage). For each measure, a model comparing light intensity, genotype, and their interaction was compared to the null hypothesis model with only light intensity. In both models an additional grouping variable was added to model effects for individual flies, such that H0: Yij = β0+β1NDi+β2Flyj+ eij and H1:Yij = β0+β1NDi+β2Genotypei+β3ND*Genotypei+β2Flyj+ eij where i

represents each trial and j represents each fly.

## Machine learning algorithm for tracing cartridges and puncta

Detecting individual cartridges was challenging due to the heterogeneity in intensity and texture within a dataset. We, therefore, trained a random forest model using 10-15 3D annotated training examples in the MATLAB-based VoxelClassifier

(https://hms-idac.github.io/VoxelClassifier/). In the training examples, background and cartridge pixels were annotated as separate classes. The features that were trained consisted of intensity derivatives, Laplacian of Gaussian kernels, steerable filters, and basic texture features such as standard deviation and entropy within a 5x5 or 11x11 neighborhood. The resulting probability class map for the cartridge (foreground class) was further processed by applying a Gaussian filter with a sigma of similar radius as a typical cartridge and identifying regional maxima in each plane. These were dilated and skeletonized to form continuous filaments along the center of each cartridge. At each pixel along each filament, we employed region growing to the outer edge of each cartridge. This was repeated at each plane until the entire structure of the cartridge had been reconstructed throughout the dataset. To find puncta, we convolved a 3D Laplacian of Gaussian filter with a sigma of 2 that approximated the radius of each puncta, and identified regional maxima. This generated candidate spots on the puncta and background. To eliminate false positives, we set a robust threshold as 4 standard deviations above the median response and masked out spots that were not within a cartridge. The remaining puncta in each cartridge were counted and exported for further analysis. We used Imaris v8 (Bitplane) to verify the accuracy of cartridge and puncta segmentation.

## QUANTIFICATION AND STATISTICAL ANALYSIS

### Quantification of L2 and L4 cell numbers

L2 and L4 cell numbers were determined blind to genotype using cell-specific genetic labeling (described above). Each cartridge in the lamina contains dendrites from a single L2 neuron and the axon/neurite of a single L4 neuron. As cartridges are regularly spaced within the lamina, L2 dendrites and L4 axons within each cartridge can be identified in cross section views of the lamina. The percentage of cartridges containing L2 or L4 neurons was determined for each optic lobe scored. The percentages for lobes of the same genotype were pooled and the average percentage was determined.

### Quantification of Brp puncta in the distal regions of lamina cartridges

Using confocal microscopy, we generated z stacks of the lamina down the long axis of lamina cartridges. Within each z stack (i.e., each optic lobe) 25 well labeled cartridges were identified and the number of Brp puncta in their distal halves was counted. The top (distal edge) and bottom (proximal edge) of each cartridge was determined by the first and last sections containing L cell processes (myrtd::TOM), respectively. The midpoint of each cartridge was then identified as the section in between the top and bottom sections. Brp puncta were counted in the sections distal to the midpoint of each cartridge. This stringent criterion was used to avoid counting L2-L4 synapses in the proximal lamina. It is likely that our quantification of distal Brp puncta is an underestimate of the number of ectopic synapses formed in the absence of DIP function. Genotypes were scored in a blind manner by three individuals, and their scores were averaged.

### Quantification of DIP-β fluorescence signal

Using Zeiss image analysis software, we quantified DIP-β signal in conditional knockdown and control brains by measuring fluorescence signal through the cartridge trajectory (3 cartridges per brain). Signal intensity values and cartridge lengths were converted to percentages by setting the highest intensity within each cartridge as 100% intensity and the full length of the cartridge as 100% distance. Statistical analysis using unpaired t tests was performed after setting uniform intervals (using the spline function on MATLAB) of 0.01% distance.

### Statistical Analysis of Brp puncta

To evaluate differences in the distal, proximal, and total number of Brp puncta between genotypes we fitted a general linear model with number of Brp puncta per cartridge as the response variable, and experiment identifier (2 levels) and genotype (7 levels) as factors (using the multicomp package of the R statistical computation software). We restricted the multiple comparison to contrasts WT versus DKO, WT versus γ +/−, WT versus γ −/−, WT versus β+/−, WT versus β−/−, DKO versus γ +/−, DKO versus γ −/−, DKO versus/ β+/−, DKO versus β−/−, γ +/− versus γ −/−, γ +/− versus β+/−, γ +/− versus β−/− versus, β+/− versus γ −/−, β−/− versus β+/−, β−/− versus γ −/−, and reported the p values of the individual contrasts.

### Statistical analysis by figure

#### *Figure 1*

(H) Optomotor index, DKO (YAd) versus CTL (YAd): p = 4.9e-37. p values were computed via rank sum test and were corrected for multiple comparisons.

(I) Phototactic choice probability, DKO (YAd) versus CTL (YAd), p = 3.3e-09. p values were computed via rank sum test and were corrected for multiple comparisons.

(J-L) p values in J-L calculated via likelihood-ratio-test of linear mixed effects models (H0: No Genotype Effect, H1: Genotype effect)

(J) $p < 0.0005$

(K) $p < 0.0005$, $p < 0.005$, $p < 0.05$

(L) $p < 0.0005$, $p < 0.005$, $p < 0.05$

(O) GLM: WT versus DKO, $p < 0.001$, WT versus β+/−, $p = 0.01938$, WT versus β−/−, $p = 0.00489$;
(P) GLM: WT versus β−/−, $p = 0.00465$;
(Q) GLM: WT versus β+/−, $p = 0.00684$, WT versus β−/−, $p < 0.001$
(R) GLM: WT versus DKO, $p < 0.001$

***Figure 2***

(D) WT versus DKO, $p < 0.0001$, unpaired t test
(E) WT versus DKO, $p = 0.1671$, unpaired t test
(F) WT versus DKO, $p = 0.0677$, unpaired t test
(G) WT versus DKO, $p < 0.0001$, unpaired t test
(H) WT versus DKO, $p = 0.5190$, unpaired t test
(I) WT versus β−/−, $p < 0.0001$, unpaired t test
(J) WT versus β−/−, $p = 0.7453$, unpaired t test
(K) WT versus β−/−, $p = 0.7449$, unpaired t test
(M) WT versus β−/−, $p = 0.0049$, unpaired t test
(N) WT versus β−/−, $p = 0.0057$, unpaired t test
(O) WT versus β−/−, $p = 0.0008$, unpaired t test

***Figure 3***

(C' and D') $p < 0.005$ from 80%–83% distance; $p < 0.0001$ from 84% −100% distance, unpaired t tests for each 0.01% distance interval.
(E and G) $p = 0.0001$, unpaired t test
(F) $p < 0.0001$, unpaired t test

***Figure 4***

(D) CTL versus R cells-DIP- γ, $p < 0.0001$, unpaired t test
(H) CTL versus L cells-DIP- γ, $p = 0.0014$, unpaired t test
(L) CTL versus L-cells-DIP- β, $p < 0.0001$, unpaired t test
Figure S1
(B) DKO (Ad) versus CTL (Ad), $p = 2.2e\text{-}05$. p values were computed via rank sum test and were corrected for multiple comparisons.
(C) DKO (YAd) versus CTL (YAd), $p = 6.7e\text{-}04$ and DKO (Ad) versus CTL (Ad), $p = 2.2e\text{-}09$. p values were computed via rank sum test and were corrected for multiple comparisons.
(F) On transient WT versus DKO, ($p = 3.3e\text{-}36$), steady state (SS) WT versus DKO, ($p = 3.6e\text{-}06$), off transient (Off) WT versus DKO ($p = 2.2e\text{-}5$).

***Figure S2***

(I) WT versus DKO, $p = 0.2090$, unpaired t test
(J) WT versus DKO, $p = 0.7053$, unpaired t test
(K) WT versus DKO, $p = 0.3840$, unpaired t test

***Figure S3***

(C'' and D'') $p < 0.05$ from 80%–100% distance, unpaired t tests for each 0.01% distance interval.

## DATA AND CODE AVAILABILITY

This study did not generate/analyze [datasets/code].

# Update

Neuron
Volume 106, Issue 2, 22 April 2020, Page 355

DOI: https://doi.org/10.1016/j.neuron.2020.04.007

Neuron
Correction

# Control of Synaptic Specificity by Establishing a Relative Preference for Synaptic Partners

Chundi Xu,* Emma Theisen, Ryan Maloney, Jing Peng, Ivan Santiago, Clarence Yapp, Zachary Werkhoven, Elijah Rumbaut, Bryan Shum, Dorota Tarnogorska, Jolanta Borycz, Liming Tan, Maximilien Courgeon, Tessa Griffin, Raina Levin, Ian A. Meinertzhagen, Benjamin de Bivort, Jan Drugowitsch, and Matthew Y. Pecot*
*Correspondence: xcd0317@gmail.com (C.X.), matthew_pecot@hms.harvard.edu (M.Y.P.)
https://doi.org/10.1016/j.neuron.2020.04.007

(Neuron *103*, 865–877.e1–e7; September 4, 2019)

The authors regret that two authors were omitted in the original published version of the manuscript. The authors apologize for this error. Also, with the unfortunate passing of Lead Contact Matthew Y. Pecot shortly after publication, correspondence can be addressed to Chundi Xu (xcd0317@gmail.com). All authors now agree to the author designations and contributions. These items have been corrected in the online version of the manuscript.